QUANTIFYING NUTRIENTS AT WISCONSIN FRESHWATER BEACHES AND DETERMINING THE MOLECULAR RESPONSE OF *E. COLI* TO NUTRIENT LIMITATION

by

Sophia Ward

A Thesis Submitted in

Partial Fulfillment of the

Requirements for the Degree of

Master of Science

in Freshwater Sciences

at

The University of Wisconsin-Milwaukee

May 2024

ABSTRACT

QUANTIFYING NUTRIENTS AT WISCONSIN FRESHWATER BEACHES AND DETERMINING THE MOLECULAR RESPONSE OF *E. COLI* TO NUTRIENT LIMITATION

by

Sophia Ward

The University of Wisconsin-Milwaukee, 2024
Under the Supervision of Professor Sandra McLellan

Escherichia coli (*E. coli*) are popular fecal indicator bacteria (FIB) used by many beach management programs in Wisconsin to evaluate the health risks posed by beaches. Prolonged survival of *E. coli* in beach sand undermines beach management practices that rely on FIB enumeration in surface water because sand and water are routinely mixed through wave action. Studies have shown that sand is a favorable environment for *E. coli* due to temperature, moisture, nutrient content, and protection from UV radiation. In addition, some sources of *E. coli* pose significantly less of a threat to human health than human fecal waste, but culture methods cannot determine the source of the pollution. In our project, we further investigated why sand serves as a favorable environment for *E. coli* through field sampling of six Wisconsin freshwater beaches throughout the Summer of 2023. We determined the *E. coli* and nutrient concentrations in berm sand and surface water samples. Overall, *E. coli* and nutrient concentrations in berm sand were not significantly different across the six beaches. However, we determined that there are large and small-scale regional factors that can cause some beaches to have high bacteria and nutrient burdens, such as rainfall, beach size, and beach topography. In addition, we examined the

molecular response of *E. coli* to nutrient modulation in beach sand using laboratory microcosms with *E. coli* constructs that produce GFP in response to nutrient limitation. The constructs were extensively validated through sequencing and microbiological techniques before deployment in microcosms. Nutrient data acquired in the first part of this study, combined with the response of the constricts in beach sand, support our determination that sand is a nutrient deficient environment for *E. coli*. The sand-model system used in this study has the potential to be used to investigate prolonged survival of *E. coli* in sand due to the presence of nutrient sources, such as the freshwater algae *Cladophora*. The results of this study not only inform the beach management programs of the sampled beaches about the *E. coli* and nutrient status of their beach, but also adds to our scientific understanding of *E. coli* survival in secondary environments.

TABLE OF CONTENTS

List of Figures vi

List of Tables vii

List of Abbreviations viii

Acknowledgements ix

Chapter 1-Introduction and literature review 1
- Section 1.1 Use of *E. coli* in water quality assessments 1
- Section 1.2 *E. coli* enumeration methods in freshwater 2
- Section 1.3 *E. coli* in survival in beach sand 3
- Section 1.4 Study objectives 4

Chapter 2- Characterization of nutrients in Wisconsin freshwater beach sand 5
- Section 2.1 Introduction 5
- Section 2.2 Methods 6
- Section 2.3 Results 16
- Section 2.4 Discussion 27

Chapter 3- Molecular response of *E. coli* reporter constructs to nutrient limitation 36
- Section 3.1 Introduction 36
- Section 3.2 Methods 37
- Section 3.3 Results 41
- Section 3.4 Discussion 48

Chapter 4- Conclusions 52

Chapter 6- References 54

Appendix A: Beach Sampling data 59

Appendix B: Spatial variation of *E. coli* and nutrient variability between sites at Simmons Island Beach in Kenosha 65

Appendix C: Medias for *E. coli* GFP construct validation 71

Appendix D: Ideal sand-model system protocol with *E. coli* GFP constructs 73

LIST OF FIGURES

Figure 1 Sampling Schedule 7

Figure 2 Map of sampled beaches in Ozaukee County 9

Figure 3 Map of sampled beaches in Milwaukee County 10

Figure 4 Map of sampled beaches in Kenosha County 11

Figure 5 Representation of a beach 12

Figure 6 Images of sampled beaches 13

Figure 7 *E. coli* concentration at Wisconsin beaches 18

Figure 8 Linear regression of pooled berm sand vs surface water *E. coli* concentrations 20

Figure 9 Linear regression of berm sand vs surface water *E. coli* concentrations at all beaches 21

Figure 10 Nutrient concentration in berm sand 23

Figure 11 Nutrient concentration in surface water 24

Figure 12 Total dissolved phosphorus concentration in berm sand 25

Figure 13 Gel electrophoresis image of PCR-amplified constructs 40

Figure 14 Fluorescence of JM109:GFP and K12 cells after extraction from sand 41

Figure 15 Fluorescence of *gln*A cells in liquid media at high and low nutrient conditions 42

Figure 16 Fluorescence of *csi*D cells in liquid media at high and low nutrient conditions 43

Figure 17 Fluorescence of *pho*A cells in liquid media at high and low nutrient conditions 44

Figure 18 Fluorescence of *usp*A cells in liquid media at high and low nutrient conditions 45

Figure 19 Fluorescence of *gln*A cells after extraction from high and low nutrient sand 46

Figure 20 Fluorescence of *csi*D cells after extraction from high and low nutrient sand 47

LIST OF TABLES

Table 1 Mean *E. coli* concentrations at Wisconsin freshwater beaches 17

Table 2 Mean nutrient concentrations in berm sand at Wisconsin beaches 26

Table 3 DOC/TDN ratios at Wisconsin Freshwater Beaches 26

Table 4 Geometric mean of *E. coli* concentrations in surface water at Wisconsin beaches during Summer 2023 30

Table 5 30-day geometric mean of *E. coli* concentrations in surface water at Wisconsin beaches during Summer 2023 31

Table 6 List of promoters attached to GFP in the constructs ordered from Horizon Discovery 36

LIST OF ABBREVIATIONS

CFU	Colony Forming Units
DOC	Dissolved organic carbon
E. coli	*Escherichia coli*
FIB	Fecal Indicator Bacteria
g	Gram
L	Liters
mL	Milliliter
MPN	Most Probable Number
NPOC	Non-purgeable organic carbon
nm	Nanometer
RWQC	Recreational Water Quality Criteria
RFU	Relative fluorescence units
TDC	Total dissolved carbon
TDP	Total dissolved phosphorus
TDN	Total dissolved nitrogen
USEPA	United States Environmental Protection Agency
µg	Microgram
ATW	Atwater Park Beach
BB	Bradford Beach
EICH	Eichelman Park Beach
HAR	Harrington State Park North Beach
PWSB	Port Washington South Beach
SIMM	Simmons Island Park Beach

ACKNOWLEDGEMENTS

I would like to extend my gratitude and appreciation for the opportunity to achieve my master's degree under my advisor, Dr. Sandra McLellan. I would also like to thank the other members of my committee, Dr. Gyaneshwar Prasad and Dr. Harvey Bootsma, whose guidance and expertise were invaluable to me during my time at the School of Freshwater Sciences. A very big thank you to Tim Wahl, who was an immense help when I was processing what seemed like an endless number of samples for nutrient analysis.

I would like to thank all the members of the McLellan Lab: Kieyarrah Dennis, Brenden Nihart, Melissa Schussman, Melinda Bootsma, and Patricia Bower. Their support and assistance, during the highs and lows of my degree, are greatly appreciated. I am also very grateful for the help I received from the undergraduate researchers in the McLellan Lab who worked tirelessly on my project with me: Kirandeep Kaur, Mariella Boudreau, Zachary Lewan, and Benjamin Gallion.

I also would like to thank Angela Schmoldt for her help in the Genomics Center, as well Karen Baumann and Anna Barnard in the Bootsma lab for their help when processing samples for total dissolved phosphorus. I am thankful for all the other faculty and staff at SFS who supported me along my journey, and my fellow classmates who made the journey more fun.

Lastly, I am forever grateful for the endless love and support I received all my life from my amazing parents; I am proud to be their daughter. I would also like to thank my partner, Liam McDonald, and all of my friends and family who stood by me and encouraged me. The funding for this project was provided by the Wisconsin Sea Grant.

Chapter 1- Introduction

1.1 Use of *E. coli* in water quality assessments

Escherichia coli are rod-shaped coliform bacteria that live in the guts of many warm-blooded animals, such as humans, ruminants, and gulls. From this primary habitat they can enter the environment, or secondary habitat, by way of feces (Walk et al., 2007). Through the lens of public health, important secondary habitats are freshwater beaches. These areas are extensively monitored for fecal pollution due to the risk it poses to human health. Humans are reservoirs for pathogens such as enteroviruses and pathogenic enteric bacteria like *Salmonella*, *Shigella* spp (Harwood et al., 2014; McLellan & Salmore, 2003). In addition, some strains of *E. coli* can cause extraintestinal infections with symptoms such as fever and diarrhea (Odonkor & Ampofo, 2013). Since *E. coli* can be grown readily in the laboratory and is inexpensive to quantify, they are fecal indicator bacteria (FIB) that are recommended for use by the United States Environmental Protection Agency (USEPA) when evaluating health risks in freshwater (US EPA, 2012). The presence of *E. coli* does not necessarily indicate that fecal pollution is present, but fecal pollution is rarely present without detecting FIBs like *E. coli* (McLellan & Salmore, 2003).

In 2000, pathogen and pathogenic indicator monitoring in recreational waters became required by law in the Federal Beach Assessment and Coastal Health (BEACH) Act. The BEACH Act was added as an amendment to the Clean Water Act (CWA) (33 U.S.C. §1313 et seq. 2000)**.** The new law allowed the USEPA to support beach monitoring and assessment programs in all states, territories, or tribes with Great Lakes beaches through grants. The grants were also intended to support development of a notification system that would inform the public of possible health risks associated with beaches. As a part of this law, the USEEPA is required to routinely publish recreational water quality criteria (RWQC) that considers the latest scientific

knowledge in the water quality assessment field. The EPA's 2012 RWQC for *E. coli* suggest a geometric mean of (GM) of 126 CFU/ 100 mL for at least five samples collected within 30 days (US EPA, 2012). When used together, the values are protective of the designated use of primary contact in fresh waters and they constrain the number of high water quality values (US EPA 2012). In Wisconsin and many other states, the DNR and local health officials monitor Great Lakes and inland beaches for pathogens using culture-based methods that rely on FIB enumeration.

1.2 *E. coli* enumeration in freshwater

More recently, molecular-based methods have been suggested to be used as an alternative to culturing. These methods include quantitative polymerase chain reaction (qPCR) which relies on targeting, extracting, amplifying, and quantifying DNA from *E. coli* (Walker et al., 2017). The resultant DNA copy numbers correlate to how much *E. coli* is present at the beach. One advantage of these methods is that they are "real-time" and are much faster than culture-based techniques, which can take about 18 hours before the results can be used to act if needed (Walker et al., 2017). However, there are certain contingencies have prevented these methods from becoming popular. First, qPCR tends to overestimate the amount of *E. coli* present in a sample because it can amplify DNA from dead, rather than live cells (Walker et al., 2017). In addition, the *Escherichia* genus is very large and diverse so choosing gene targets that are ubiquitous but specific to *E. coli* is difficult and if chosen incorrectly can result in co-amplification of closely related species (Walker et al., 20017). Lastly, these methods are more difficult to implement since they would require the development of new standardization and data acceptance criteria (Shanks et al., 2016).

Many current beach monitoring tactics that rely on *E. coli* enumeration using culture-based techniques cannot distinguish the source of the bacteria, which means the type of pollution that may be present cannot be differentiated. The presence of human fecal pollution at beaches is usually the result of rare regional contamination events such as sewage overflows (McLellan & Salmore, 2003). Combined sewer overflows (CSOs) and sanitary sewer overflows (SSOs) can occur after heavy rainfall events and are associated with increases in gastrointestinal illnesses (Templar et al., 2016). Non-point sources and agricultural runoff can also impair water quality because they dump fecal waste, inorganic pollutants such as nitrogen, and organic pollutants such as pesticides into surface waters (Kumwimba et al., 2018).

1.3 *E. coli* in beach sand

Evidence shows that most *E. coli* are from waterfowl feces, not sewage contamination (Edge & Hill, 2006; Safaie et al., 2021). In a study done by Cloutier & McLellan (2017), host-associated fecal markers were used to examine the source of *E. coli* at beaches in Milwaukee, Sheboygan, and Manitowoc counties. The gull-associated marker for *Catellicoccus marimammalium* (Gull2) was detected more frequently than any other host-associated marker. It was present in a significant amount of sand and water samples with the highest *E. coli* levels. Both human-associated markers were found to be present at much lower levels than Gull2. Although water contaminated with bird and other animal feces can also cause disease in humans, it is to a much lesser extent.

Studies also show that sand is a favorable environment for *E. coli* survival and promotes *E. coli* persistence, and in some cases growth, long after a pollution event has occurred (Alm et al., 2006; Beversdorf et al. 2007; Cloutier & McLellan, 2015). This contrasts with the earlier hypothesis that secondary habitats like beach sand expose pathogens to many harmful stimuli

including UV radiation, temperature fluctuations, and low concentrations of nutrients which creates a hostile environment (Walk et al., 2007). Therefore, survival and growth of *E. coli* in the beach sand environment complicates beach monitoring practices, which rely on *E. coli* enumeration in the nearby surface water and do not examine the sand.

1.4 Study objectives

This study had two major objectives. The first was to determine the range, if any, of *E. coli* and nutrient concentrations in berm sand and nearby surface water at six Wisconsin freshwater beaches during the Summer of 2023. While sampling, sanitary surveys were performed and saved in the EPA's Survey123 app to determine possible sources of nutrients at the beach. Berm sand and surface water samples were collected, prepped, stored, and analyzed for *E. coli*, nitrogen, carbon, and phosphorus concentrations. Then, the *E. coli* and nutrient concentrations at each beach were compared through data analysis.

After determining the nutrient concentrations in the sand at the beaches, the molecular response of *E. coli* to nutrient limitation was determined through microbiological and sequencing techniques. Four *E. coli* constructs that produce GFP in response to carbon, nitrogen, and phosphorus limitation were ordered from Horizon Discovery and validated extensively. Once validated, they were deployed in laboratory microcosms that represent the beach environment to determine the molecular response of *E. coli* to nutrient concentrations in real Wisconsin beach sand.

Chapter 2- Characterization of nutrients in Wisconsin freshwater beach sand

2.1 Introduction

In a study on *E. coli* in sand done by Beversdorf et al. (2007), it was found that sand provides ample protection for the bacterium from UV radiation and a favorable environment in terms of nutrient levels. Nutrients that are necessary for microbial survival include carbon, nitrogen, and phosphorus. Another study evaluated the effects of carbon/nitrogen ratios on *E. coli* survival using laboratory microcosms. They found that high carbon/nitrogen ratios, or increased carbon levels compared to nitrogen, prolonged *E. coli* survival above baseline levels, while low carbon/nitrogen ratios had no effect (Meyers & McLellan, 2022). Other studies have found that lower carbon/nitrogen ratios resulted in *E. coli* cell loss in microcosm studies with compost, but this could also be explained by a lower total amounts of available nutrients (Somorin et al., 2016; Mandel & Silhavy, 2005). Due to these discrepancies in the literature, the effect of nutrients on *E. coli* survival in sediment needs to be investigated further.

Another reason for the prolonged survival of *E. coli* in beach sand is due to the presence of *Cladophora* species. *Cladophora* are algae that commonly exist in freshwater streams and lakes. They grow in the form of dense strands and mats that attach to hard substrates but are often dislodged and can end up decaying on the banks of rivers and the shores of lakes (Byappanahalli et al., 2003). This causes aesthetic and odiferous issues for beach managers and visitors to the beaches. It is also well documented that the mats carry large concentrations of attached *E. coli* which in turn increases *E. coli* concentrations in nearshore waters (Byappanahalli et al., 2003). In addition, the presence of *Cladophora* in sand prolongs the survival of *E. coli* at higher concentrations than in the nearby water (Byappanahalli et al., 2003). The exact mechanisms behind the beneficial relationship between *Cladophora* and *E. coli* are

unknown, but it is believed that the algae provide the bacteria with protection from UV radiation and nutrients in its leachate (Zhang et al., 2021; Beckinghausen et al., 2014). In Meyers & McLellan (2022), results suggest that fresh *Cladophora* has a higher potential to release nutrients over time than already decayed mats. Common beach management practice is usually to remove the *Cladophora* mats as soon as they end up on the beach, although this doesn't always happen (Bootsma, 2004).

Due to wave action, *E. coli* populations in the sand are continuously dispersed throughout the nearby water column which increases concentrations in the water even with no recent pollution events (Brown & Boehm, 2016; Byappanahalli et al., 2003; Cloutier & McLellan, 2017; Staley et al., 2018; Whitman & Nevers, 2003; Whitman et al., 2003; Vogel et al., 2016). Just the *E. coli* concentration alone does not contain any information about the source of the bacteria, which can be from numerous sources: gulls, *Cladophora* algal mats, humans, or other mammals. Not knowing the source of the bacteria can lead beach managers to make misleading decisions that impact public health (Field & Samadpour, 2007; Staley & Edge, 2016). Understanding the mechanisms behind *E. coli* survival in freshwater beach sand, especially in the context of nutrient provision, can help inform culture-based *E. coli* enumeration techniques for water quality assessments.

2.2 Methods

Beach surveying

The sampled beaches are located along the shore of Lake Michigan in Wisconsin. They are in 3 different counties: Ozaukee, Milwaukee, and Kenosha. Figure 2 shows the locations of Harrington State Park North Beach (HAR) and Port Washington South Beach (PWSB) which were sampled in Ozaukee County. Figure 3 shows the locations of Atwater Park Beach (ATW)

and Bradford Beach (BB) which were sampled in Milwaukee County. Lastly, Figure 4 shows the locations of Simmons Island Park Beach (SIMM) and Eichelman Park Beach (EICH), which were sampled in Kenosha. Pictures of all the sampled beaches are shown in Figure 6. Milwaukee beaches were sampled at least 10 times while Kenosha and Ozaukee beaches were sampled at least nine times according to the sampling schedule in Figure 1.

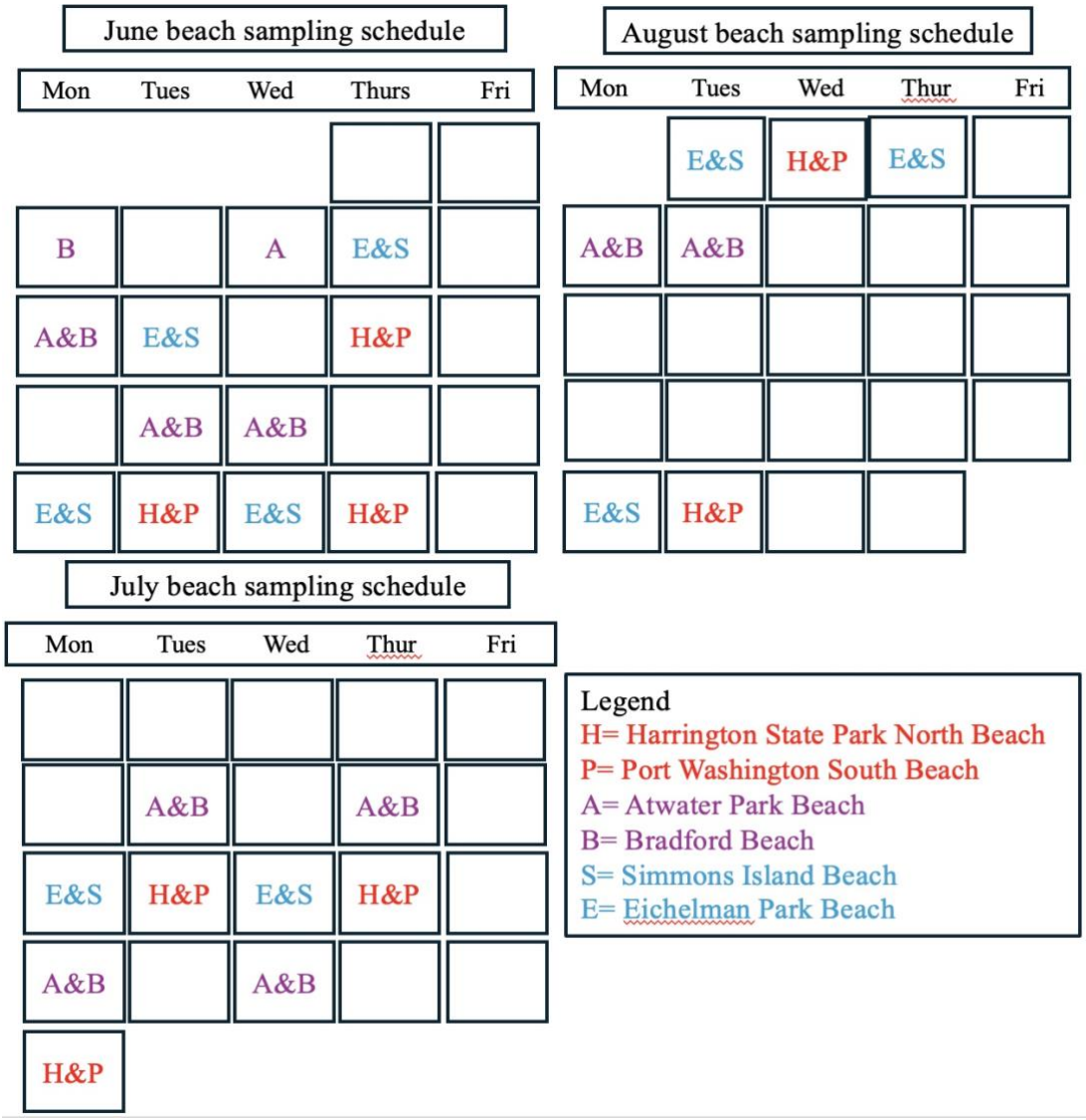

Figure 1. Beach sampling schedule by month during the summer of 2023. Two sampling events to Ozaukee beaches also took place at the end of May (05-24-2023 and 05-30-2023) but are not included in this figure.

At every beach, samples were collected at three different sites (except for Atwater Beach, which has four sites) which were denoted as Site 3, Site 2, and Site 1, respectively. Sites were chosen so that they are roughly equally spaced along the length of the beach. Site 1 is the most southern site while Site 3 is the most northern site at each beach. Coordinates for each site from the McLellan lab were used. Site coordinates were determined upon the first sampling event at the beaches that did not have recorded site coordinates in the McLellan lab. For each sampling event, sanitary survey data was collected in the Sanitary Survey App for Marine and Fresh Waters developed by the EPA. This app was accessed through the Survey123 app which was pre-downloaded onto a smartphone. This app allows for easy compilation, storage, and analysis of sanitary survey data. The person/people who sampled filled out the survey while sampling to the best of their abilities and uploaded pictures when appropriate. Data that was logged in the survey included air temperature, wave height and frequency, water odor and color, and recent rainfall, along with the presence of algae, wildlife (dead and/or alive), humans, and any outfalls or nearby structures that may affect the status of the beach. Observations were made visually or by using local weather station websites.

Figure 2. Map of beaches in Ozaukee County. Harrington State Park North and Port Washington South Beach are marked with a yellow star (WDNR, Ozaukee County Beaches, 2017).

Figure 3. Map of beaches Milwaukee County. Atwater Park Beach and Bradford Beach are marked with a yellow star (WDNR, Milwaukee County Beaches, 2015).

Figure 4. Map of beaches Kenosha County. Simmons Island Park Beach and Eichelman Park Beach are marked with a yellow star (WDNR, Kenosha County Beaches, 2017).

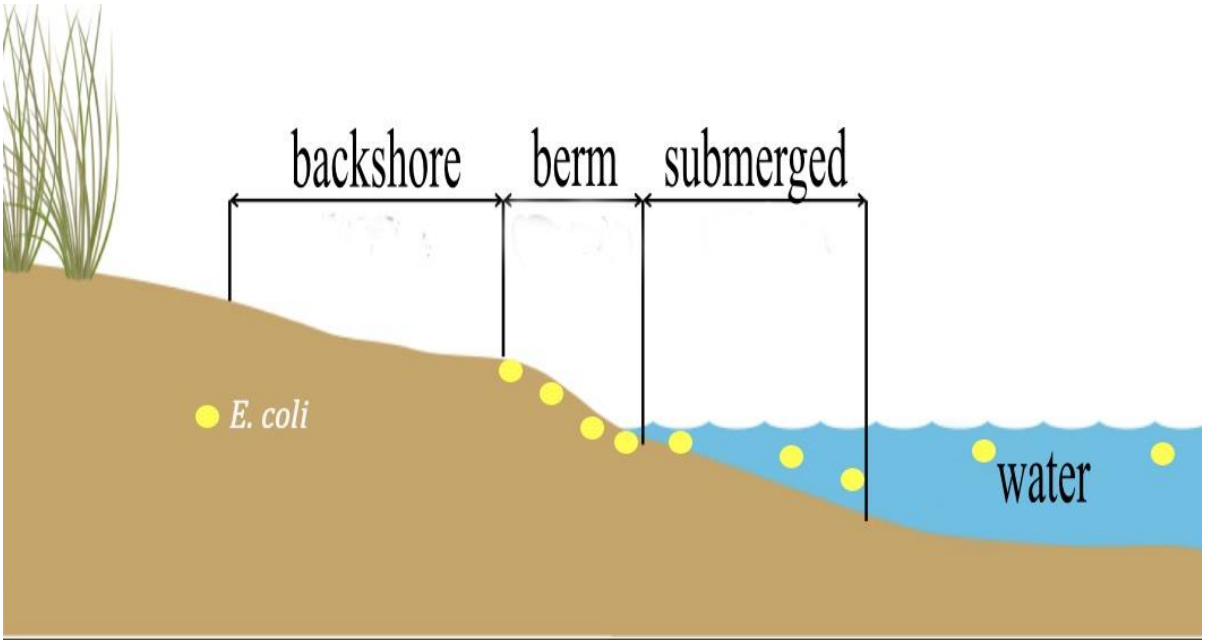

Figure 5. Representation of *E. coli* reservoirs at a beach (Adapted from McLellan & Prasad (n.d.))

While at each site, surface water and berm sand samples were collected. Surface water samples were collected in 500 mL Nalgene bottes using a sampling pole. At each site, water was collected at least two to three feet below the surface. The bottles were washed out three times before they were filled and capped. The sampler was careful not to touch the inside of the cap or bottle while taking each sample to prevent phosphorus contamination from their skin. For the sand samples, the sampler filled a whirlpack with sand from the berm region of the beach, which is pictured in Figure 5. The size of this area varies by beach but is recognizable since the sand in this region is intermittently wetted due to wave action. Both the sand and water samples were labeled with the date, beach, and site number. All samples were kept in a cooler until they were brought back to the lab, where they were kept at 4 °C until processing.

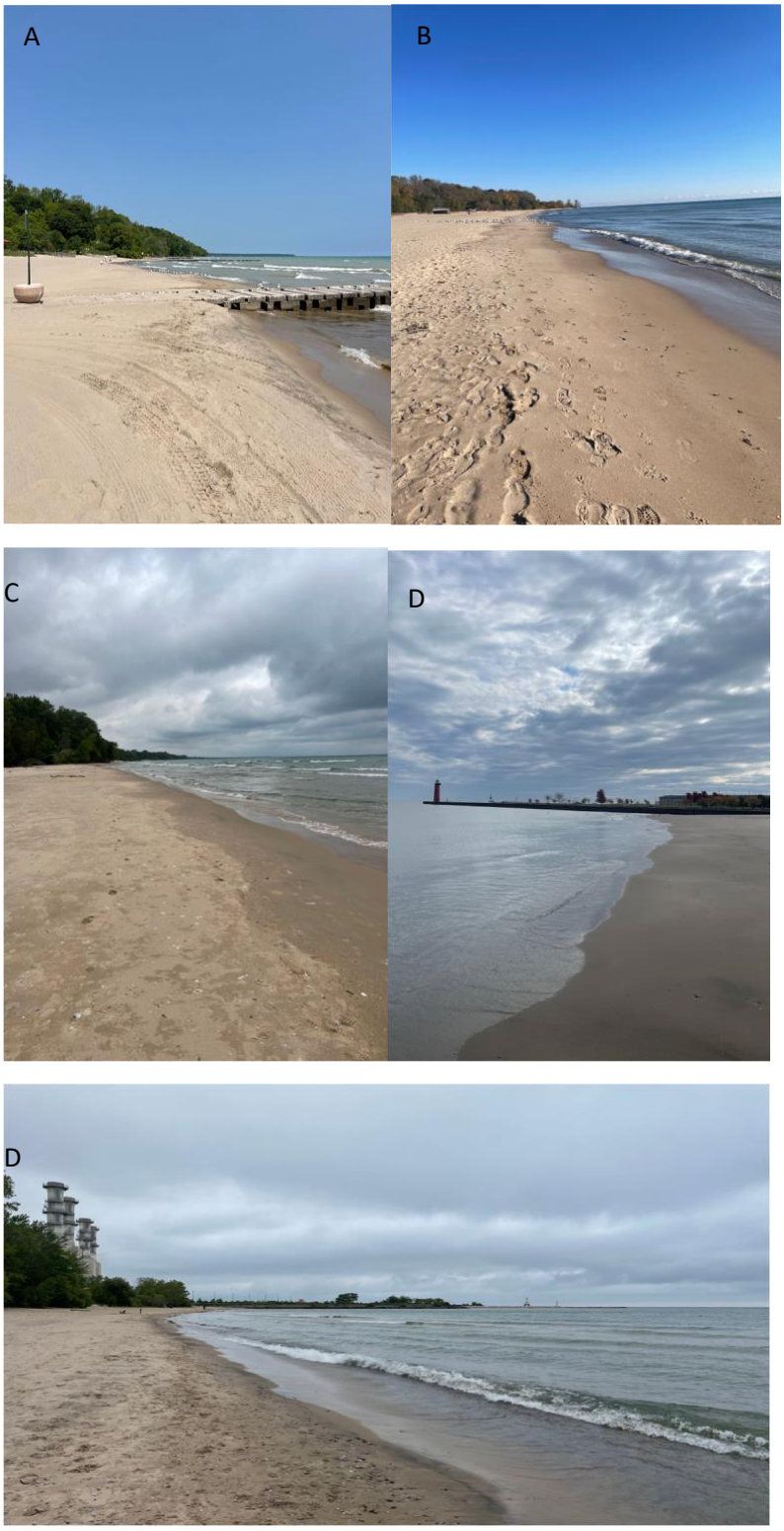

Figure 6. Images of sampled beaches. Atwater Park Beach (A), Bradford Beach (B), Harrington State Park North Beach (C), Simmons Island Beach (D), and Port Washington South Beach (D). Eichelman Park Beach is not pictured.

Sample processing

Upon return to the lab, plates were prepared of the water and sand samples for *E. coli* enumeration. For the water samples, 100 mL was filtered through 0.45-µm-pore-size nitrocellulose filters (0.47-mm diameter/; Millipore, Billerica, MA), placed on modified mTEC agar, and incubated for 2 hours at 36 °C then 18-22 hours at 44 °C. Sand was mixed with water at a 1 g: 10 mL ratio and 100 mL was filtered and plated similar water sample processing. After 24 hours of incubation, the plates were counted for colony forming units (CFU). If the plate count is too high to reliably count, then it was replated at an appropriate volume. The water and sand samples mentioned above were also filtered through 0.22-µm-pore-size nitrocellulose filters (0.47-mm diameter/; Millipore, Billerica, MA) and the filters were immediately frozen at -80 °C for later microbial community analysis.

Lastly, water and sand samples were prepared for nutrient analysis. Before filtering, the filters were pre-washed with 400 mL of MilliQ water to wash any carbon or nitrogen from the filter. The sand was mixed at a ratio of 16 g: 40 mL DI water with a total of 32 g sand and 80 mL MilliQ water. All samples and MilliQ blanks were filtered through 0.22-µm-pore-size mixed cellulose ester (MCE) filters (0.47-mm diameter/; Millipore, Billerica, MA). The filtrates were collected in 50 mL falcon tubes and stored at -20 °C until analyzed.

Nutrient analysis

Carbon and nitrogen concentration analysis was done using the Shimadzu TOC Analyzer with the TN extension located in the Analytical Lab. For total dissolved carbon (TDC) analysis, 1 mL sample was pipetted into a 15 mL falcon tube along with 9 mL of MilliQ water. Tubes were inverted three times to mix the samples, which were then transferred to washed and

combusted 10 mL glass vials. For total dissolved organic carbon (DOC) and simultaneous total dissolved nitrogen (TDN) analysis, 10 mL of the sample was pipetted into 15 mL falcon tubes along with 25 mL of 10% HCl solution. The tubes were inverted three times to mix the sample and transferred to glass vials. Standards for the carbon calibration curves ranged from 0.5-10 ppm carbon while the standards for the nitrogen calibration curve ranged from 0.5-5 ppm nitrogen.

Data from the Shimadzu TOC Analyzer is reported in milligrams TDC/DOC/TDN per liter of sample. The reported concentration of TC was multiplied by 10 before converting to micrograms TDC/DOC/TDN per milliliter of water/gram of sand. For sand samples, the dilution ratio was also considered in order to convert to micrograms TDC/DOC/TDN per gram of sand.

Methods from Stainton et al. (1977) were used to determine the total dissolved phosphorus (TDP) concentration of the sand samples. This method relies on the photo-oxidation of organic phosphorus into orthophosphate using a short UV irradiator. Once converted, the orthophosphate concentration can be measured using the same adapted method that measures soluble reactive phosphorus (SRP). In acidic conditions, phosphate will react with molybdate to form compounds which can be reduced by ascorbic acid to form a blue-colored complex. The intensity of this blue color is therefore proportionate to the concentration of phosphate in a sample and can be measured with a UV spectrophotometer.

Data analysis

All data visualization and statistical analysis was performed using RStudio, version 2023.12.1+402. *E. coli* concentrations were $\log_{10}$-transformed before analysis. The Shapiro-Wilk test was used at $p<0.05$ to assess the normality of *E. coli* and nutrient concentrations. The *E. coli*

concentration in surface water data, the total dissolved carbon and nitrogen in sand data, and the TDN/TDP ratio data was normal, so a two-way analysis of variance (ANOVA) was performed at $p<0.05$ to determine significant differences by beach. If a significant p-value was obtained, post hoc analysis was done using Tukey Honestly Significant Difference (HSD) at $p<0.05$ to determine which beaches differed significantly from each other. The *E. coli* concentrations in sand data, the total dissolved organic carbon concentration in sand, the nutrients in water data, and the DOC/TDN and DOC/TDP ratios were not found to be normal. Therefore, a Kruskal-Wallis analysis was performed at $p<0.05$. Post hoc analysis was done with Dunn's test at $p<0.05$ to determine which beaches differed significantly from each other if a significant p-value was obtained. Lastly, the Mann-Whitney test was used to compare the beginning and end of the summer *E. coli* concentrations at $p<0.05$ to determine if the *E. coli* concentrations at the end of the summer were significantly higher.

2.3 Results

E. coli concentrations at Wisconsin beaches

Berm sand *E. coli* concentrations differed significantly from each other among beaches at $p<0.05$. Post hoc analysis with no p-value adjustment showed that EICH sand had significantly higher *E. coli* concentrations than ATW, BB, and SIMM at the level of $p<0.05$. EICH sand also had significantly higher *E. coli* concentrations than HAR at $p<0.005$ and PWSB at $p<0.0005$. Beaches EICH and SIMM are the only beaches within the same region that had significantly different sand *E. coli* concentrations. However, the mean sand concentration at EICH is within the same log as the mean sand concentration at SIMM (Table 1). Water *E. coli* concentrations did not differ significantly from each other by beach at $p<0.05$ ($p=0.496$). The range of *E. coli* concentrations in the sand and water at the sampled beaches is depicted in Figure 7.

Table 1. Mean *E. coli* concentrations at the sampled Wisconsin freshwater beaches. Concentrations were log-transformed before they were averaged.

Beach	Mean *E. coli* concentration in sand (Log(CFU/g sand) ± SD)	Mean *E. coli* concentration in surface water (Log(CFU/100 mL) ± SD)
HAR	0.934 ± 0.883	1.547 ± 0.844
PWSB	0.557 ± 0.374	1.208 ± 0.594
ATW	1.178 ± 0.843	1.595 ± 0.524
BB	1.079 ± 0.548	1.364 ± 0.646
SIMM	1.114 ± 0.701	1.283 ± 0.312
EICH	1.926 ± 0.741	1.670 ± 0.539

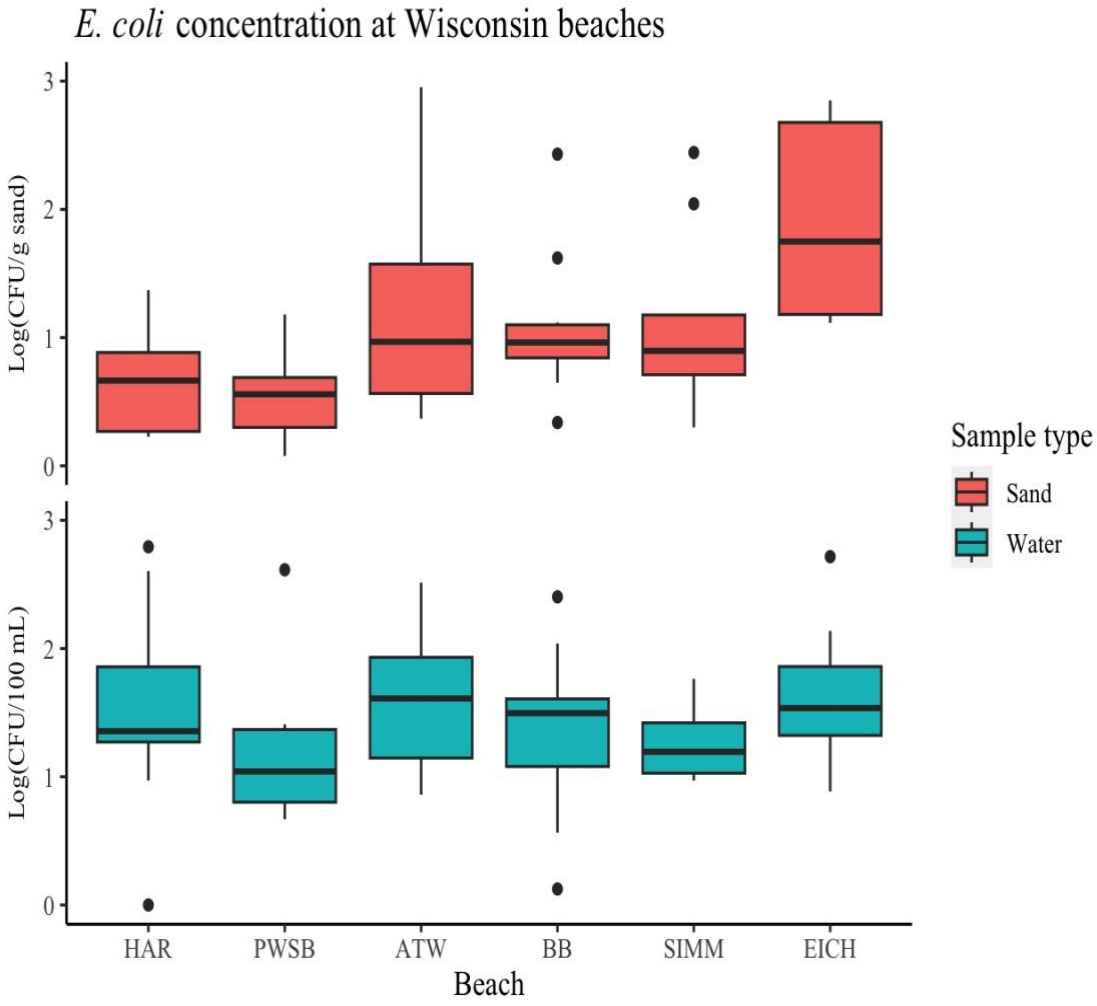

Figure 7. Boxplots of the *E. coli* concentration in the sand and surface water at the sampled beaches (n=10 for Milwaukee beaches and n=9 for Ozaukee and Kenosha beaches). *E. coli* data was log-transformed before plotting. Black dots represent outliers. EICH had significantly higher berm sand *E. coli* concentrations than all beaches at he level $p<0.05$. Surface water *E. coli* concentrations were not significantly different from each other at $p<0.05$.

Linear models were made to determine if berm *E. coli* concentrations are reliable indicators of nearby surface water *E. coli* concentrations at each beach and overall (Figures 8 & 9). Several studies have shown that *E. coli* in berm sand is dispersed throughout the nearby water column through wave action (Staley et al., 2018; Cloutier & McLellan, 2017; Brown & Boehm, 2016; Vogel et al., 2016; Byappanahalli et al., 2003; Whitman & Nevers, 2003; Whitman et al., 2003). ATW, PWSB, and SIMM models had significant p-values at $p<0.0001$ and $p=0.05$, respectively. The pooled data also showed a significant positive relationship between berm sand and surface water *E. coli* concentrations at $p<0.0001$. For all beaches individually and pooled together there is a positive relationship between sand and water *E. coli* concentrations, indicated by positive slopes.

E. coli has also been shown to have the ability to replicate in beach sand and is constantly deposited into this environment, lending evidence to the hypothesis that *E. coli* accumulates in beach sand over the summer. To investigate this, a linear regression was performed with sand *E. coli* data over the summer at each beach, and with all the beach data pooled together. No significant p-values were observed at the level of $p<0.05$, and the slope of PWSB was negative (-9.91×10^{-4}). Beginning and end sand concentrations were compared to each other at each beach to see if the sand concentrations at the beaches were significantly higher at the end of the summer. No significant p-values were observed at the level of $p<0.05$.

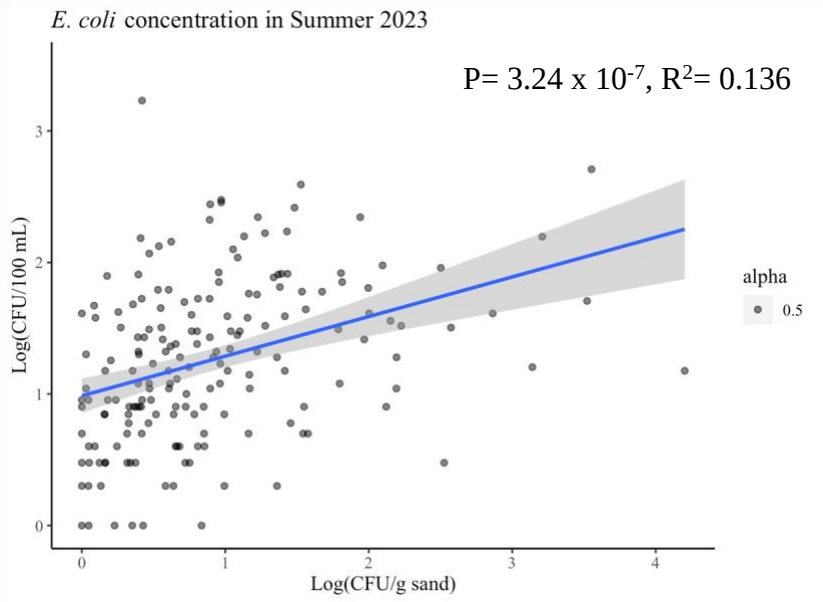

Figure 8. Linear regression of berm sand (x-axis) vs surface water *E. coli* concentrations (y-axis) at all beaches for all sampling events. A significant positive relationship is observed at the level of $p<0.0001$.

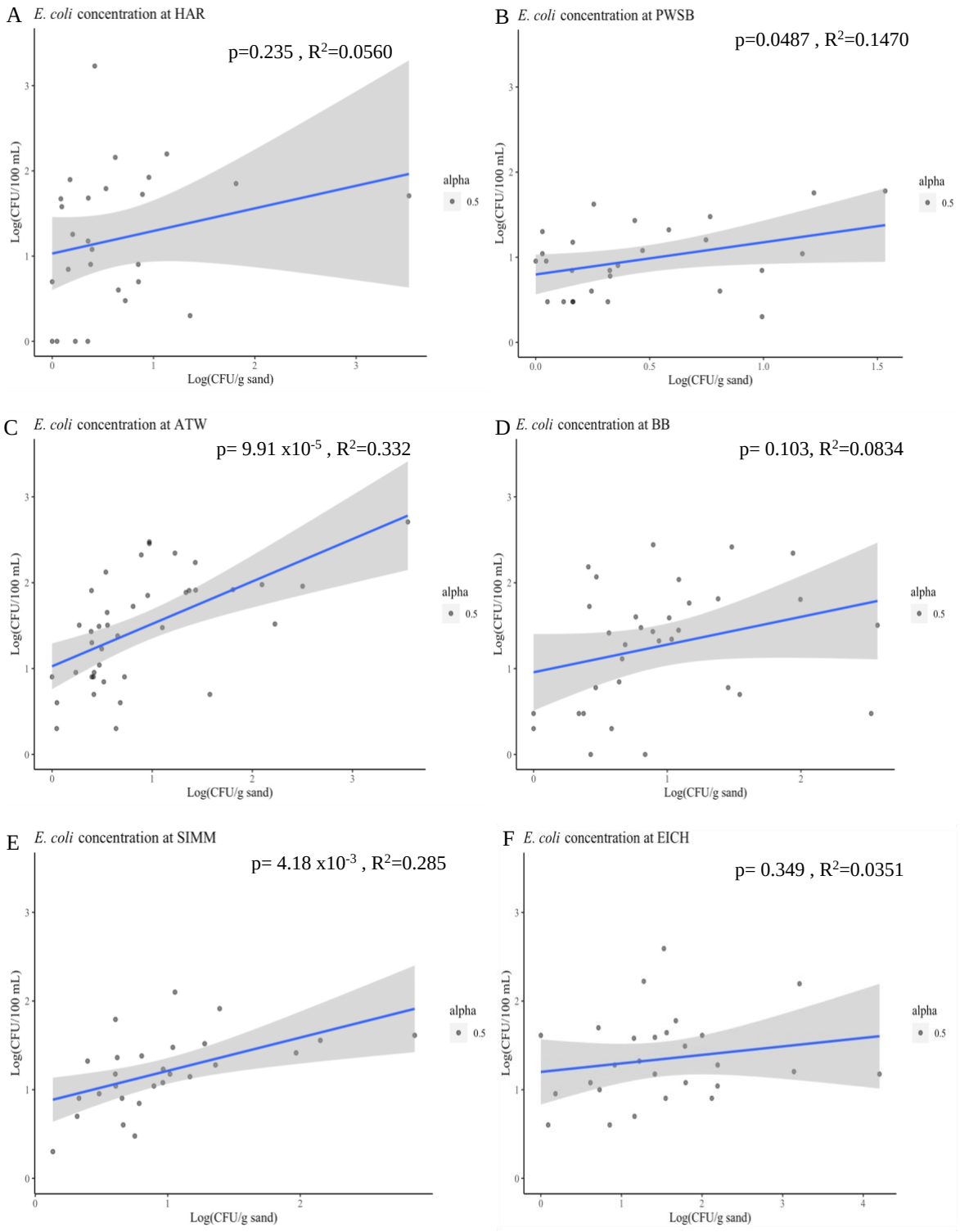

Figure 9. Linear regressions of berm sand (x-axis) vs surface water *E. coli* concentrations (y-axis) at HAR (A), PWSB (B), ATW (C), BB (D), SIMM (E), and EICH (F). A significant positive relationship is observed for PWSB, ATW, and SIMM models, but a positive relationship is seen for all beaches.

Nutrient concentrations at Wisconsin beaches

The range of nutrient concentrations in berm sand are shown below in Figure 10. Berm sand TDC, DOC, and TDN concentrations were not significantly different from each other at $p<0.05$ ($p=0.480$, $p=0.256$, and $p=0.0589$). Both the Milwaukee beaches had relatively high carbon concentrations in sand, with BB having the highest average TDC and DOC concentrations overall. However, Dunn's post hoc analysis showed that EICH had a significantly higher DOC concentration than PWSB and a higher TDN concentration than PWSB and ATW at $p<0.05$. Sand TDN data was normal, but the p-value was very close to $p<0.05$ so both an ANOVA and Kruskal Wallis test with post hoc analysis was preformed to determine if there were significant differences among beaches. Tukey's post hoc analysis showed no significant differences at $p<0.05$. Water TDC, DOC, and TDN concentrations were also not found to be significantly different from each other at $p<0.05$ and are shown in Figure 11.

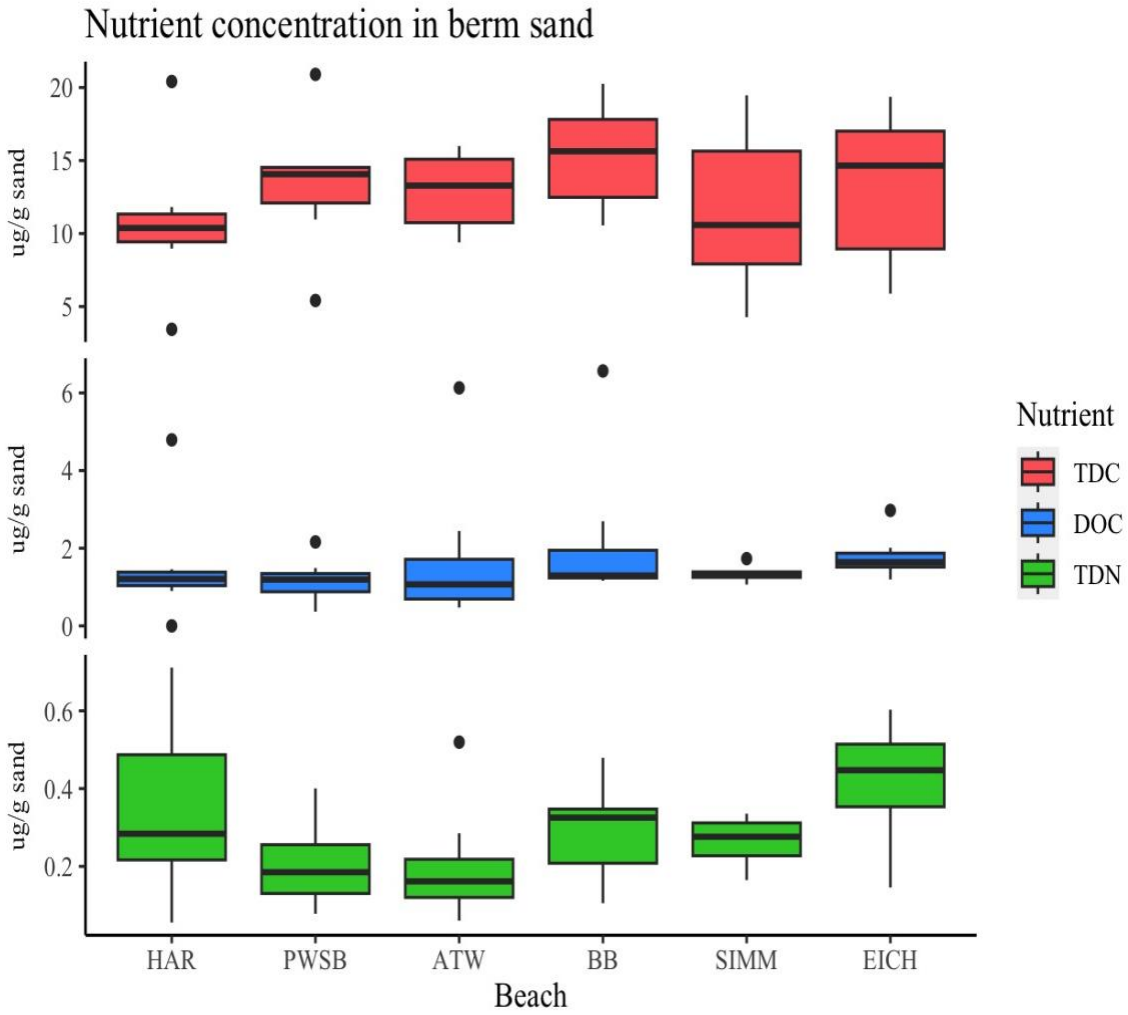

Figure 10. Nutrient concentration of berm sand at the sampled beaches (n=8 for Milwaukee beaches and n=7 for Ozaukee and Kenosha beaches). Boxplots represent the total dissolved carbon, total dissolved organic carbon, and the total dissolved nitrogen in berm sand in units of microgram per gram of dry sand. Black dots represent outliers.

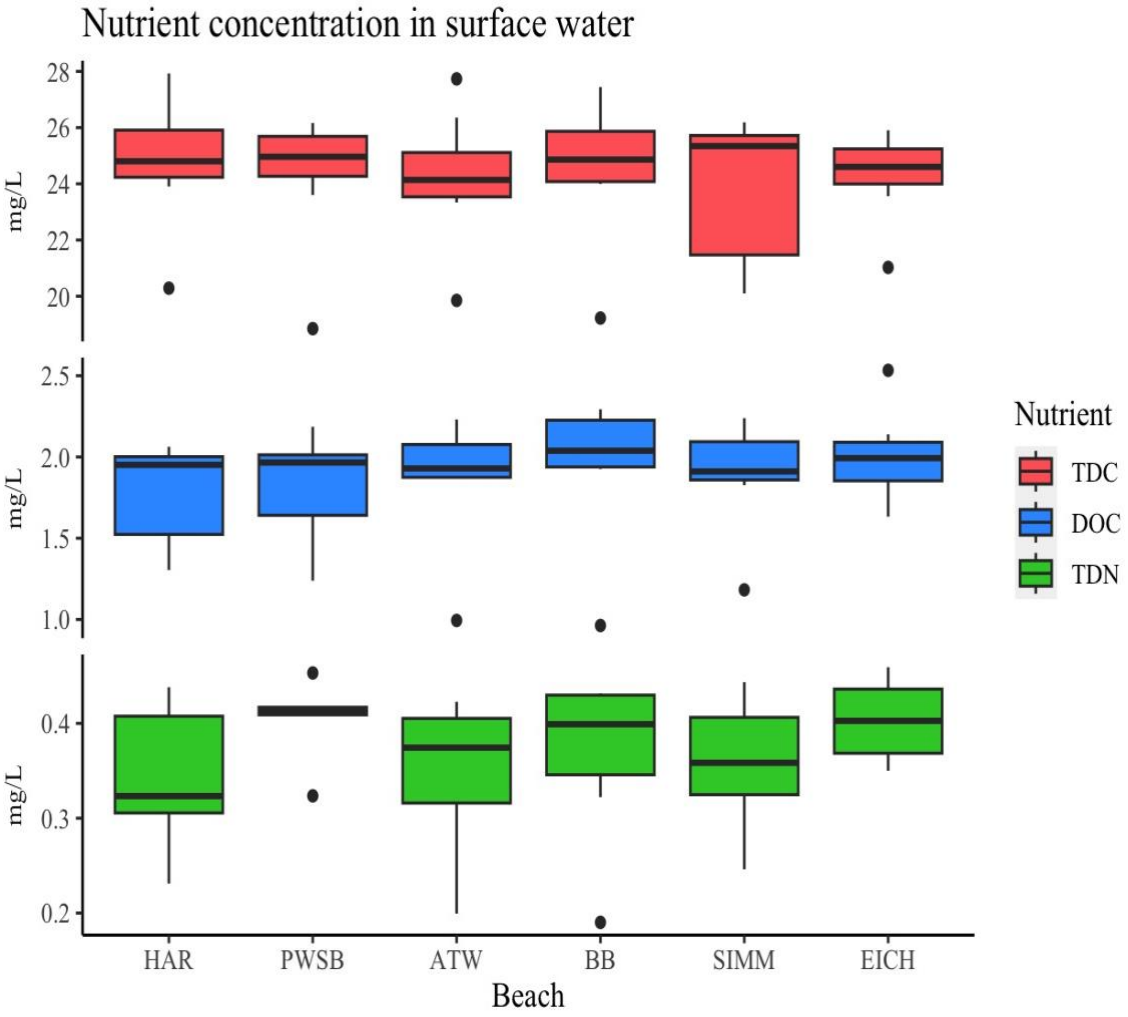

Figure 11. Nutrient concentration of surface water at the sampled beaches. (n=8 for Milwaukee beaches and n=7 for Ozaukee and Kenosha beaches). Boxplots represent the total dissolved carbon, total dissolved organic carbon, and the total dissolved nitrogen of surface water in units of milligrams per liter. Black dots represent outliers. No significant differences were observed among beaches at the level of $p<0.05$.

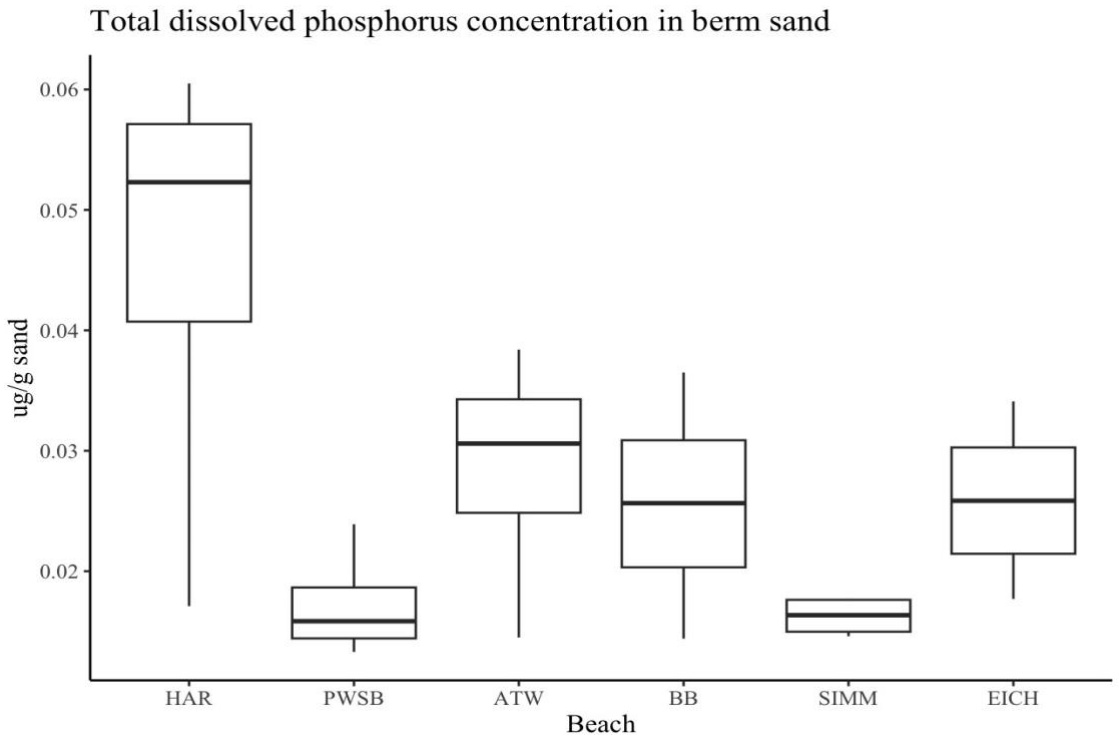

Figure 12. Total dissolved phosphorus concentration in berm sand. Boxplots represent TDP in micrograms per gram of dry sand. Four sampling events were analyzed for each: one event in the beginning, two events in the middle, and one event at the end of the sampling season (n=4). EICH had significantly higher TDP than PWSB and ATW at the level of $p<0.05$.

Berm sand TDP concentrations were also not found to be significantly different from each other at $p<0.05$. However, Figure 12 shows that HAR sand had the highest median TDP. In addition. Dunn's post hoc analysis showed that HAR had a significantly higher TDP concentration than PWSB and SIMM at $p<0.05$. Table 2 shows a summary of the mean TDC, DOC, TDN, and TDP concentrations in berm sand at all the sampled beaches.

Table 2. Mean nutrient concentrations in berm sand at the sampled Wisconsin beaches. Nutrient concentrations are in units of micrograms per gram of dry sand.

Beach	Mean TDC ± SD (μg/ g sand)	Mean DOC ± SD (μg/ g sand)	Mean TDN ± SD (μg/ g sand)	Mean TDP ± SD (μg/ g sand)
HAR	10.82 ± 5.03	1.549 ± 1.509	0.351 ± 0.232	0.046 ± 0.020
PWSB	13.37 ± 4.64	1.167 ± 0.564	0.205 ± 0.110	0.017 ± 0.005
ATW	12.88 ± 2.68	1.749 ± 1.884	0.202 ± 0.145	0.028 ± 0.010
BB	15.38 ± 3.49	2.146 ± 1.856	0.291 ± 0.121	0.026 ± 0.009
SIMM	11.63 ± 5.56	1.341 ± 0.205	0.265 ± 0.066	0.016 ± 0.002
EICH	13.12 ± 5.21	1.798 ± 0.578	0.419 ± 0.154	0.026 ± 0.007

Table 3. Mean nutrient ratios in sand and water at sampled beaches. Sand and water nutrient concentrations were converted to units of mmol/L before the ratios were calculated.

Beach	Surface water DOC/TDN ratios	Berm sand DOC/TDN ratios	Berm sand DOC/TDP ratios	Berm sand TDN/TDP ratios
HAR	6.266	6.485	99.181	20.371
PWSB	5.156	10.500	173.388	27.228
ATW	6.301	9.797	185.507	21.344
BB	6.208	9.516	295.006	30.912
SIMM	6.184	6.717	191.950	30.350
EICH	5.802	5.839	216.380	43.016

DOC/TDN ratios were not found to be significantly different from each other by beach in sand at $p>0.05$. Interestingly, BB and ATW had the most similar DOC/TDN ratios in sand and water to each other while the ratios differed more among the other beaches within the same county as each other. In addition, DOC/TDP and TDN/TDP ratios were not found to be significantly different from each other by beach in sand at $p<0.05$. The ratios from each beach are shown in Table 3 and are mostly consistent with the 106: 16: 1 ideal ratio of carbon, nitrogen, and phosphorus in marine microorganisms determined in 1940 by R.H. Fleming, although most beaches have slightly elevated carbon levels (Geider and La Roche, 2002).

2.4 Discussion

E. coli survival dynamics in the beach environment is a poorly understood phenomenon. Prolonged survival of *E. coli* in sand confounds traditional beach monitoring practices that rely on *E. coli* enumeration in nearby surface water because the *E. coli* in the sand, that may not be from a recent pollution event, is continuously mixed with the surface water. Many factors could influence the amount of *E. coli* that is deposited at a beach and the ability for *E. coli* to persist in the sand, including rain events, water temperature wave intensity, presence of wildlife feces, and *Cladophora* mats (Byappanahalli et al., 2003; Whitman & Nevers, 2003; Abia et al., 2015; Vogel et al., 2016; Cloutier & McLellan, 2017). These factors can change annually, making some beaches more prone to harboring *E. coli* than others during different years. One of the aims of our study was to extensively monitor *E. coli* concentrations at Wisconsin beaches to understand how these smaller and larger-scale regional factors affect *E. coli* burdens at these beaches. Overall, there were not significant differences in *E. coli* concentrations in sand or surface water by beach. In addition, we analyzed nutrient concentrations in the sand and water to

determine if there is a strong correlation with *E. coli* burdens. Overall, the beaches were not significantly different from each other in terms of nutrient concentrations. However, like *E. coli* concentrations, there are small-scale regional factors that can moderately affect the amount of carbon, nitrogen, and phosphorus in sand and nearby surface water. The conclusions of this study are not only informative to beach management programs in Wisconsin, but they are also informative to our general understanding of *E. coli* persistence in a secondary environment such as beach sand.

E. coli concentration in Eichelman Park Beach sand

Overall, *E. coli* sand concentrations did not differ significantly from each other by beach. EICH berm sand had the highest average *E. coli* concentrations out of all the beaches, suggesting that some beaches are more prone to high *E. coli* burdens than others. This is most likely due to small-scale regional factors, such as the construction of the beach. EICH is the smallest beach sampled, just 0.129 miles in length (Wisconsin DNR, Beaches List, 2023). It also has a breakwater constructed on the North end of the beach that extends into the water. This area, which is Site 3, is prone to collecting algal mats and attracting waterfowl species. Although these features are not necessarily unique to EICH, its small size may lead to concentration of *E. coli* compared to the other sampled beaches. In addition, the breakwater may allow for recirculation of the *E. coli* that is exchanged with the water back into berm sand.

High *E. coli* concentrations in berm sand align with the high number of exceedances, advisories, and closures at EICH during Summer 2023. The Beach Monitoring and Notification program run by the Wisconsin DNR posts advisory signs for beaches when the *E. coli* concentration exceeds 235 CFU (or MPN)/100 mL for a single sample or a geometric mean of

126 CFU/100 mL for 5 samples collected within 30 days (Magee, & Packett, 2022). Geometric means of surface water *E. coli* concentrations at the sampled beaches using data collected in this study and data provided by the DNR are listed in Tables 4 & 5. Beaches are closed when *E. coli* concentrations exceed 1000 CFU/100 mL (Magee, & Packett, 2022). Out of the 44 *E. coli* concentration reports made for EICH in 2023, there were 6 instances where the concentrations exceeded 235 CFU/100 mL resulting in an exceedance percentage of 13.64% (Wisconsin DNR, Beach Reports, 2023). EICH was also closed due to elevated bacteria levels twice, which is the most out of any beach. Similarly to EICH, SIMM had the second highest exceedance rate at 7.5% and was closed once due to elevated *E. coli* levels (Wisconsin DNR, Beach Reports, 2023).

We did notice some regional patterns in *E. coli* concentrations, where beaches that are closest to each other have similar highs and lows. This relationship was also shown in a five year study of 23 Chicago beaches by Whitman and Nevers (2008), where spatial autocorrelation was observed for *E. coli* concentrations in surface water at beaches that were closest together regionally. According DNR Beach Report data, EICH and SIMM had the highest number of exceedances, advisories, and closures due to elevated bacteria in 2023. Both beaches also have recreational impairments due to elevated *E. coli* levels according to the WI DNR (Wisconsin DNR, Impaired Water Search, 2024). However, according to Tables 4 and 5, surface water geometric means from our surface water data or DNR data does not indicate that either beach is impaired during the Summer of 2023. HAR and ATW only had one exceedance and advisory due to elevated bacteria, while PWSB and BB had none. HAR also has a recreational use impairment because of elevated *E. coli* levels, while ATW and BB were delisted in 2012 and PWSB is not listed. According to Tables 4 and 5, none of the beaches are impaired during the Summer of 2023. In addition, none of the beaches had any closures due to elevated bacteria.

Table 4. Geometric mean of surface water samples at Wisconsin beaches during the Summer of 2023. Geometric means were calculated using surface water data collected in this study as well as reports published by the DNR from 05/30/2023 to 08/28/2023 (Wisconsin DNR, Beach Reports, 2023).

Sample type	HAR	PWSB	ATW	BB	SIMM	EICH
Water (CFU/100 mL)	17.0	7.8	26.8	16.1	14.0	20.5
DNR (MPN/100 mL)	45.0	9.9	28.3	44.7	48.7	60.8

Using DNR data, we also noticed larger-scale regional patterns in *E. coli* concentration fluctuations year to year. Whitman and Nevers (2008) also showed that all 23 Chicago beaches exhibited similar temporal fluctuations in surface water *E. coli* concentrations, suggesting that larger-scale regional factors also play a role. One such larger-scale regional factor is precipitation. Several studies have shown the link between heavy rainfall and increased *E. coli* concentrations in surface water at beaches (Kleinheinz et al., 2009; Haack et al., 2003; Scopel et al., 2003). We also noted year-to-year differences in water quality. According to DNR Beach report data, there were more exceedances and closures in 2022 for all the sampled beaches due to elevated bacteria than there were in 2023. In addition, there were more exceedances at all beaches in 2022 than there were in 2021. National Weather Service precipitation data showed that 2022 had higher average precipitation in all counties with sampled beaches during May, June, July, and August than in 2021 and 2023 (National Weather Service, 2024). In 2021 there was an average of 0.11 inches of rainfall, while there was an average of 0.077 inches in 2021 and 0.089 inches in 2023 (National Weather Service, 2024). Annually, there was higher or equal

average rainfall in all counties in 2022 compared to 2021 and 2023 (National Weather Service, 2024).

Table 5. Geometric mean of at least five surface water samples collected within 30 days at Wisconsin beaches during the Summer of 2023 and data from reports published by the DNR from 05/30/2023 to 08/28/2023 (Wisconsin DNR, Beach Reports, 2023).

Sample type	HAR[1]	PWSB[1]	ATW	BB	SIMM[1]	EICH[1]
Water 1				9.4		
Water 2			36.7	25.3		
DNR 1	26.4	8.3	19.8	52.6	33.7	44.7
DNR 2	51.0	10.0	35.2	35.1	41.6	37.0
DNR 3	48.3	9.4	22.2	36.0	61.7	96.6

Footnote[1]: There were not at least five samples taken within a 30 day period for these beaches in our study, so 30-day geometric means were not determined using our data.

E. coli concentrations in beach sand and surface water

In this study we enumerated *E. coli* concentrations in berm sand and nearby surface water determine if there is a positive relationship between them. Overall, there is a positive linear relationship at each sampled beach and in pooled sand and water data. The relationships at some beaches are stronger than others, but this is consistent with other studies that have found significant positive relationships between berm sand and nearby surface water quality (Phillips et al., 2011; Skalbeck et al., 2010; Zehms et al., 2008). Factors that can affect this relationship include rain, wind patterns, and wave intensity. Vogel et al. 2016 showed a positive relationship between wave height and release of *E. coli* from berm sand. In addition, they investigated the difference in the release of *E. coli* from sand at beaches with different sand types. At finer sand

beaches, sand erosion from wave activity increases transfer of *E. coli* to nearby surface waters while they found that interstitial pore water flow and discharge is more likely strongly related at coarser sand beaches.

We also used our data to determine if *E. coli* accumulates in beach sand over the course of the summer. Other studies have noticed temporal variability over small amounts of time and seasonal variability in beach sand (Zehms et al., 2008; Vogel et al., 2016). *E. coli* concentrations are typically lower at the end of the winter, but they start to increase in the spring when the snow melts (Zehms et al., 2008). Our data didn't show any significant positive relationship over the summer at the individual beaches or pooled together, but it does not mean that this relationship doesn't exist. More intensive sampling overall and a longer sampling season would certainly help examine this relationship further. Starting sampling in March or April and continuing sampling until late September or October would be ideal. For this study, beaches were only sampled until August, and the Ozaukee and Kenosha beaches were only sampled once during the last week of August. Like all studies, there are limitations to the amount of sampling that can be done due to a multitude of reasons, including funding availability and personnel availability.

Range of nutrients at Wisconsin beaches

Overall, there were no significant differences in nutrient concentrations in the sand or water at the sampled beaches. Interestingly, the Milwaukee beaches both had relatively high TDC and DOC concentrations in sand whereas this was not the same for other beaches in the same region. This could possibly be due to urban regional factors, since Ozaukee and Kenosha counties are much less urbanized according to the maps of each county in Chapter 1 of this study. In addition, there were other differences that could be explained by smaller-scale

regional factors, including beach size and topography as well as pollution from agricultural runoff.

EICH sand had the highest overall *E. coli* concentration in berm sand. In addition, EICH sand had relatively high DOC and TDN concentrations, except for TDP. Although SIMM is located within a mile of EICH, the same pattern of *E. coli* and nutrient concentrations was not observed there. SIMM had relatively low DOC and TDN concentrations compared to EICH, and had the second lowest average sand *E. coli* concentration. This suggests that some beaches are more prone to higher nutrients and *E. coli* concentrations than others, possibly due to beach-specific features such as size and topography. SIMM is over four times the size of EICH (Wisconsin DNR, 2023 Wisconsin Beaches List). There is also a breakwater that was constructed near Site 1 at EICH. This, combined with EICH's small size, most likely contributes to both phenomena and allows for constant recirculation of nutrients and *E. coli* at the beach. Although surface water *E. coli* concentrations were not found to be significantly different from each other, EICH also had the highest *E. coli* concentration in surface water as well.
We also noticed that some beaches were prone to high TDN and TDP concentrations in berm sand, possibly because of pollution from agricultural runoff. Agricultural nonpoint surface runoff has been implicated as a major problem for Great Lakes watersheds and can cause a myriad of problems, including the eutrophication of streams, rivers, and lakes (Kerr et al., 2016). Due to manure and fertilizer application, agricultural runoff can load organic nitrogen and phosphorus into beach environments which can lead to water quality impairments (Kerr et al., 2016). HAR sand had the highest TDP concentration and the second highest TDN concentration.

The high nitrogen and phosphorus concentration at HAR may be due to contamination from Sucker Creek, which is 10.19 mile river that runs parallel to the Lake Michigan shoreline

(WI DNR, Impaired Water Search, 2024). According to Google Maps, Sucker Creek is about 1.6 miles away from HAR, and it empties into Lake Michigan about 5.2 miles south of the beach. According to the WI DNR, Sucker Creek is considered impaired due to high phosphorus concentrations. A study done by the WI DNR that took the form of total maximum daily load (TMDL) development for the Northeast Lakeshore area, including Sucker Creek, quantified phosphorus loading into the watershed by source. Baseline total phosphorus loads at the mouth of Sucker Creek was 4,588 pounds per year, with 4,303 of those pounds from agricultural sources (WI DNR, 2023, The Northeast Lakeshore TMDL). Although a TMDL was not developed for nitrogen, the study also investigated nonpoint loading of nitrogen in the Northeast Lakeshore area. They concluded that there was more nitrogen being loaded into the watershed than was being removed and that the main sources of nitrogen were from nonpoint source pollution from manure and fertilizer application (WI DNR, 2023, Nitrogen in Northeast Lakeshore study area).

Interestingly, PWSB is located directly south of the mouth of Sauk Creek, which is also considered impaired by the WI DNR due to high phosphorus concentrations but has relatively low sand TDN and TDP concentrations compared to HAR and the other beaches (WI DNR, Impaired Water Search, 2024). According to the same Northeast Lakeshore TMDL study mentioned above, baseline total phosphorus loading at the mouth of Sauk Creek was 2,360 pounds per year, with 1,682 pounds from agricultural sources (WI DNR, 2023, The Northeast Lakeshore TMDL). Although the Sauk Creek outfall is directly north of PWSB, the nutrients that are loaded from the creek may be prevented from being deposited in PWSB sand because of the marina that is built around the mouth of the river. In addition, the Coal Dock Park Prairie Restoration Marker and the Port Washington Avian Sanctuary, which are located directly north

of PWSB and in between the mouth of Sauk Creek, essentially act as a breakwater and prevent the nutrient-dense water from circulating at the beach.

High TDN and TDP concentrations were not associated with high *E. coli* concentrations according to our study, indicating that dissolved nutrients alone are not dominant determinates of *E. coli* burdens at beaches. More likely, high *E. coli* concentrations are due to the large and small-scale regional factors mentioned in this section, such as rainfall and beach size and topography. Breakwaters can have powerful effects on the nutrient and *E. coli* burdens at beaches, which is evidenced by *E. coli* and nutrient patterns at beaches such as EICH and PWSB. In addition, particulate nutrients may play a role in modulating *E. coli* survival in sand but were not evaluated in this study.

Chapter 3- Molecular response of *E. coli* to nutrient limitation

3.1 Introduction

Prolonged survival of *E. coli* in secondary environments is poorly understood. This study hoped to investigate this phenomenon, more specifically how nutrients modulate *E. coli* survival in beach sand. The first objective of this study used field and laboratory techniques to determine the *E. coli* and nutrient concentrations in sand and water from six Wisconsin beaches. In the second part of this study, we used the collected nutrient data to investigate the molecular response of *E. coli* to nutrient limitation in beach sand through laboratory microcosms. To do this we ordered GFP-producing *E. coli* reporter constructs from Horizon Discovery. The constructs consist of promoter regions that control pathways that respond to nutrient stress fused to green fluorescent protein (GFP). Promoter regions are listed below in Table 6 (McLellan & Prasad, n.d.):

Table 6. List of promoters that are attached to GFP in the constructs ordered from Horizon Discovery.

Promoter name	**Description**	**Function**
*gln*A	glutamine synthetase (2nd module)	uses ammonia from amino acid degradation to form glutamine; is expressed in response to nitrogen deficiency
*csi*D	conserved protein (2nd module)	is expressed exclusively in response to carbon starvation in concert with RpoS (the general stress response signal factor) and cAMP-CRP
*pho*A	alkaline phosphatase	enzyme that cleaves phosphomonoester bonds; is expressed in response to phosphate starvation
*usp*A	universal stress protein A	expressed in response to many stresses, expect cold shock; this includes carbon and phosphate starvation

The *csi*D, *pho*A, and *usp*A constructs are in in *E. coli* K12 strain MG1655. The *gln*A construct was transformed into *E. coli* NCM3722 cells (Prasad et al, 2005). Both strains are laboratory strains.

3.2 Methods

Construct extraction and sequencing

All construct inserts were extracted using the Qiagen Spin Miniprep Kit and sent to The University of Illinois for Sanger DNA Sequencing with primers 1, 5′-CCATTAACATCACCATCTAA-3′, and 2, 5′-CCAGCTGGCAATTCCGACGT-3. Sequences from the University of Illinois were aligned using DNAStar. Extraction products were also PCR-amplified at 95 °C for 10 min, then 25 cycles of 95 °C for 30 s, 60 °C for 1 min and 72 °C for 1 min, and a final step at 72 °C for 5 min (Zaslaver, et al., 2006). PCR products were then ran on a 1.1% agarose gel using GelRed dye.

Validation of the sand experimental system with GFP-producing E. coli

E. coli JM109 cells were transformed with a plasmid that was ordered from Clonetech Laboratories and contained uvGFP. The transformed cells were used as a positive control in this experiment because they constitutively produce GFP. *E. coli* JM109:GFP and K12 cultures were grown from single colonies in LB broth overnight with 50 µg/mL ampicillin and 20 µL of Isopropyl ß-D-1-thiogalactopyranoside (IPTG) added to the JM109 culture. *E. coli* K12 cells, which do not produce GFP, were used as a negative control. The cultures were then washed two times with 0.8% NaCl before resuspension in sterile water. The optical densities (OD) were measured at 600 nm using a Synergy H4 Multi-mode Reader. The cell concentration for each culture, using the value 1 OD= $8x10^8$ cells/mL, was calculated as well as the amount of each

culture that was added to 35 g of sand collected from Bradford Beach to get a final concentration of about 10^7 cells/mL. To assess the background fluorescence of sand, an equal amount of water was added to a separate Nalgene bottle with 35 g sand. The bottles were shaken vigorously for two minutes before the sand was put into petri dishes and placed in microcosm chambers made up of a clean plastic bin with wetted paper towels to maintain moisture. The chamber was then chilled in the fridge at 18°C for an hour.

To extract the cells, 350 mL of MilliQ water was mixed with the sand from each dish in separate Nalgene bottles and shaken vigorously for two minutes. After the bottles were allowed to rest for 30 seconds, the water was decanted into centrifuge bottles and centrifuged for 8 minutes at 8000 rpm. After centrifugation the supernatant was poured off and the pellet was resuspended in 5 mL of sterile water. The resuspended pellet was pipetted into a clear 96 well plate as well as a black and white 96-well isoplate. The OD and fluorescence of the cultures was measured using a Synergy H4 Multi-mode Reader. The OD was measured at 600 nm and the fluorescence was measured at an excitation at 395 nm and emission at 510 nm with the gain set to 75.

Validation of reporter constructs in liquid culture

To validate that the constructs produce GFP when in nutrient-stressed environments, *gln*A, *csi*D, *pho*A, *usp*A, and K12 were grown in duplicate from isolated colonies in M9 media at 37 C and 250 rpm overnight. *E. coli* K12 was used as a negative control. For the reporter constructs, kanamycin was added to a final concentration of 25 μg/mL. After 16-20 hours of growth, the reporter construct cultures were diluted at a ratio of 1:10 into new full-strength and modified M9 medias that had low concentrations of carbon, nitrogen, or phosphorus (Appendix

C). K12 cells were diluted into full-strength M9 media. The OD and fluorescence was measured initially and at three subsequent time points: 7 hours, 24 hours, and 48 hours after initial dilution using a Synergy H4 Multi-mode Reader. The OD was measured using a clear 96-well plate and the fluorescence was measured in a black and white 96-well isoplate. The OD was measured at 600 nm while the fluorescence excitation was set to 485 nm and the emission was to 535 nm with the gain at 75.

Microcosms with E. coli GFP reporter constructs

Further validation was completed to ensure that the constructs respond to nutrient limitation in sand. Validation was done separately for *gln*A and *csi*D. There were two treatment types: high nutrients and native sand. The negative control treatment group consisted of K12 cells with nutrients and un-inoculated native sand was also processed to account for any background fluorescence. All treatment groups were prepared in duplicate. *Gln*A, *csi*D, and K12 cultures were grown in duplicate from isolated colonies in M9 media at 37 C and 250 rpm overnight. For the reporter construct cultures, kanamycin was added to a final concentration of 25 μg/ mL. During the *gln*A validation, all cultures were washed three times with 0.8% NaCl and resuspended in sterile water before adding to sand. Cultures were not washed during the *csi*D validation. The OD of each culture was determined before adding to sand.

Cultures were added to sand at a concentration of about 10^7 cells/g wet sand. Nutrients were added to the nutrient treatment groups in the form of M9 media (Appendix C). For the *gln*A validation, 50 μL M9 media was added to 70 g sand for each treatment group. For the *csi*D validation, 500 μL M9 media and 50 μL 20 % glucose was added to 80 g sand for each treatment group. Native sand with no additional nutrients was used for the low nutrient sand treatment

group and sterile water was added to adjust the moisture content. The sand was then homogenized and weighed into 35 mm x 10 mm petri dishes so that they contained about 30-45 g of sand. Dishes were placed in clean, loosely tented plastic containers with wetted paper towels to maintain moisture. The plastic containers were then placed in a fridge set to 18 °C until processing.

During processing, the sand from each dish was scooped into clean 500 mL Nalgene containers with 300 mL MilliQ water. Each bottle was shaken vigorously for 2 minutes, then decanted into 250 mL centrifuge bottles. The bottles were centrifuged at 3500 rpm for 17 minutes. The supernatant was poured off and the pellet was resuspended in 3 mL sterile water. Lastly, the OD was measured using a clear 96-well plate and the fluorescence was measured in a black and white 96-well isoplate. The fluorescence excitation was set to 485 nm and the emission was at 535 nm with the gain set to 97 for the *gln*A extraction and 100 for the *csi*D extraction. The OD and fluorescence of *csi*D was taken 5 hours after the cells were seeded into sand, while *gln*A was measured after 24 hours.

Data analysis

All data visualization and statical analysis was performed using RStudio, version 2023.12.1+402. A Shapiro-Wilk test was used at $p<0.05$ to assess the normality of the fluorescence intensities. Fluorescence intensities for each treatment was compared using a Kruskal-Wallis test at $p<0.05$. Post hoc analysis was done with a Dunn's test at $p<0.05$ to determine which treatments differed significantly from each other.

3.3 Results

Construct extraction and sequencing

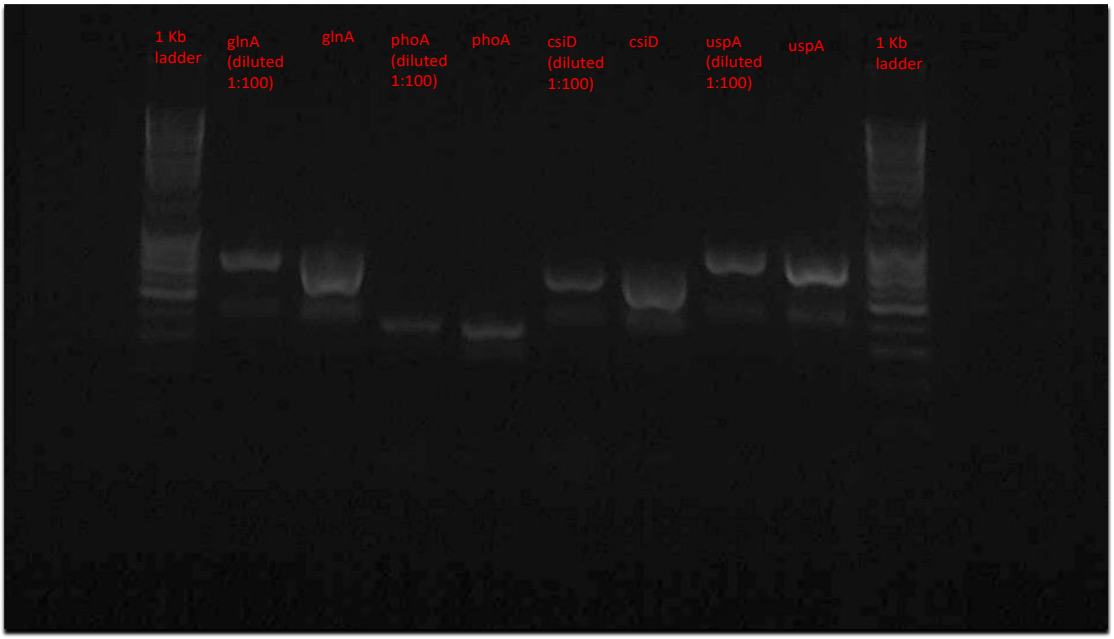

Figure 13. Image of the PCR-amplified reporter construct inserts on 1.1% agarose gel prepared using GelRed. 1 Kb ladders are located on the far left and right sides of the gel.

All extracted construct inserts appeared as bands on the gel, pictured above in Figure 13. All constructs also showed GFP in the amplified region of their DNA.

Validation of the sand-model system with JM109-GFP

To validate that a measurable GFP signal can be obtained from GFP-producing *E. coli* cells after extraction from sand, positive and negative control *E. coli* strains were deployed in a small microcosm. JM109:GFP had the highest observable fluorescence at about 144876 ± 1735 RFU, which was about 28 times higher than K12 fluorescence and 38 times higher than the background fluorescence of sand, which is denoted as the Water treatment in Figure 14. K12 had an average fluorescence of about 5140 ± 218 RFU and Water had average of about 3845 ± 704

RFU. Significant differences between the observed fluorescence were found at $p<0.005$. Using Dunn's post hoc analysis, JM109-GFP showed significantly higher fluorescence than K12 and Water at $p<0.05$ and $p<0.0005$, respectively. Water and K12 fluorescence was not significantly different from each other at $p<0.05$.

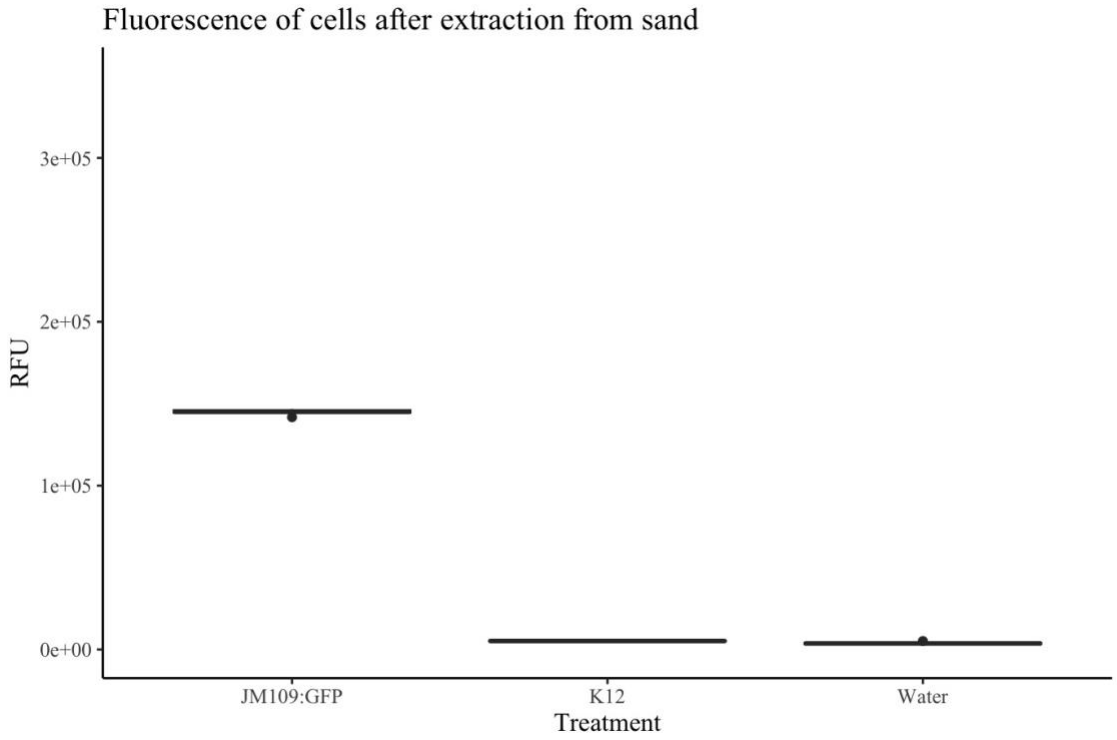

Figure 14. Boxplot of the fluorescence of JM109:GFP and K12 cells after extraction from sand. Fluorescence is in units of RFU and was normalized to OD before plotting (n=6). Fluorescence from JM109:GFP cells was significantly higher than both K12 and Water treatments.

Construct response to nutrient limitation in liquid culture

To validate the reporter constructs they were deployed in liquid culture with modified medias that contained low amounts of the nutrients to induce a GFP response and the fluorescence was measured at several timepoints. At 0 hours the fluorescence of constructs in low media is roughly the same as the fluorescence of the constructs in high nutrient media and K12. However, *gln*A and *usp*A in low phosphorus media had significantly higher fluorescence

than K12 at $p<0.0001$ and at $p<0.05$, respectively. The *pho*A also had significantly higher fluorescence than K12, but the p-value was extremely close to 0.05 ($p=0.0493$). The *usp*A in low phosphorus media also had significantly higher fluorescence than and *usp*A in high nutrient media at $p<0.05$. From 0 to 7 hours the fluorescence of all constructs and K12 generally decreases, but the difference in fluorescence of the constructs in low nutrient media and high nutrient media increases.

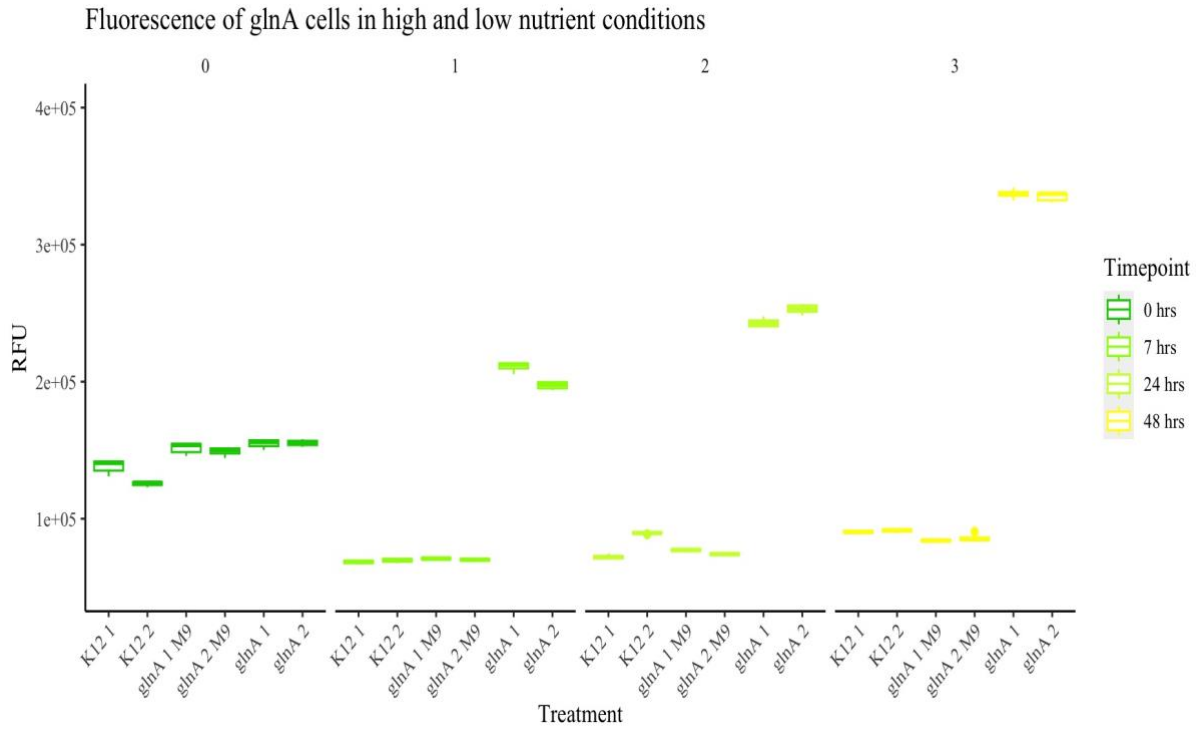

Figure 15. Boxplots of the fluorescence of *gln*A cells in liquid culture in high and low nutrient conditions. Fluorescence is in units of RFU and was normalized to OD before plotting. Outliers are represented by dots (n=6). *Gln*A in low nutrient media fluoresced the most out of all constructs at 48 hours and began fluorescing at 7 hours. At 48 hours, *gln*A in low nutrient media fluoresced about 4 times higher than *gln*A in high nutrient media.

The highest measurable GFP signal was from *gln*A at 48 hours in low nutrient media, shown in Figure 15 (336100 ± 3263 RFU). This was about 4 (3.95) times higher than the fluorescence observed from *gln*A in high nutrient media and 3.7 (3.70) times higher than K12. The biggest differences in fluorescence between low nutrient media and high nutrient media was at 7 hours for all other constructs (Figures 16, 17, & 18). The average difference in fluorescence between the constructs in low nutrient media and high nutrient media is 1.530 times higher, while it is 1.804 times higher when *gln*A data is included. The average difference in RFU between constructs in low nutrient media and K12 is 1.62 times higher, while it is 1.89 times when *gln*A data is included.

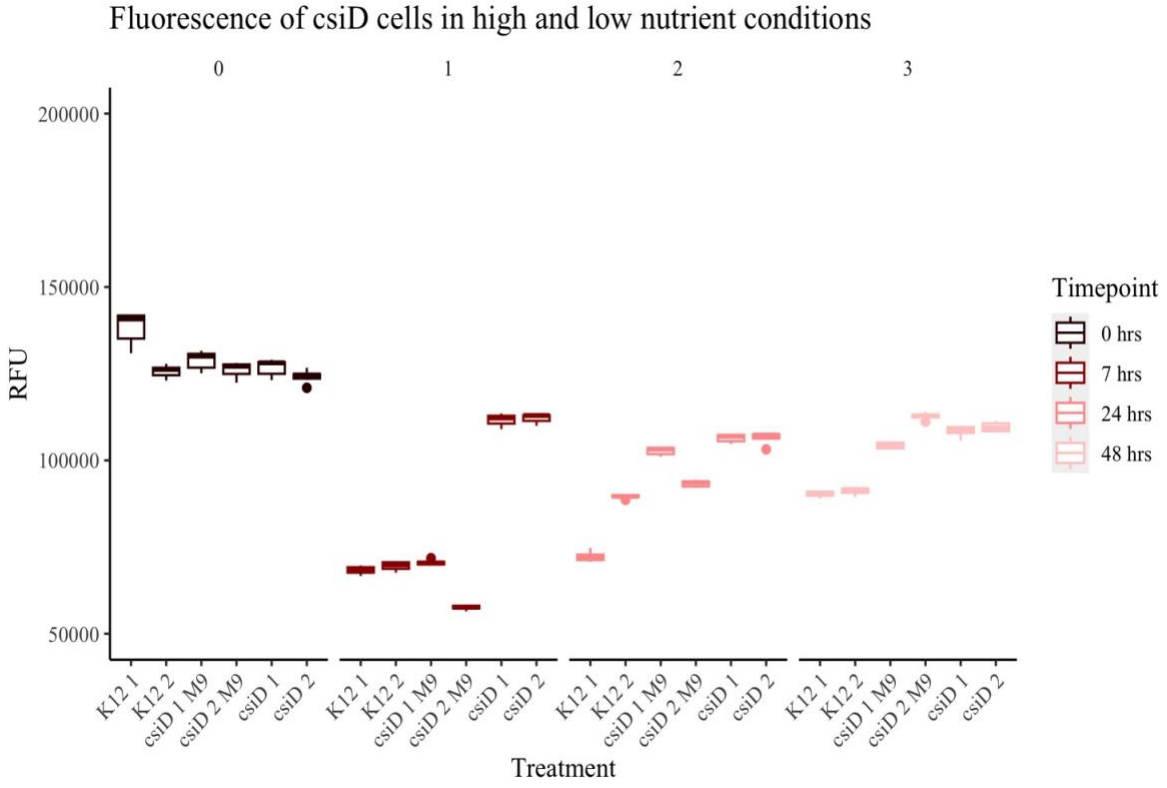

Figure 16. Boxplots of the fluorescence of *csi*D cells in liquid culture at high and low nutrient conditions. Fluorescence is in units of RFU and was normalized to OD before plotting. Outliers are represented by dots. (n=6). *Csi*D cells in low nutrient media fluoresced the highest at 7 hours, but after 7 hours *csi*D cells in high nutrient media began to fluoresce.

After 7 hours, the RFU of the constructs in the high nutrient media begins to increase, indicating that the cells become nutrient stressed after 7 hours and before 24 hours.

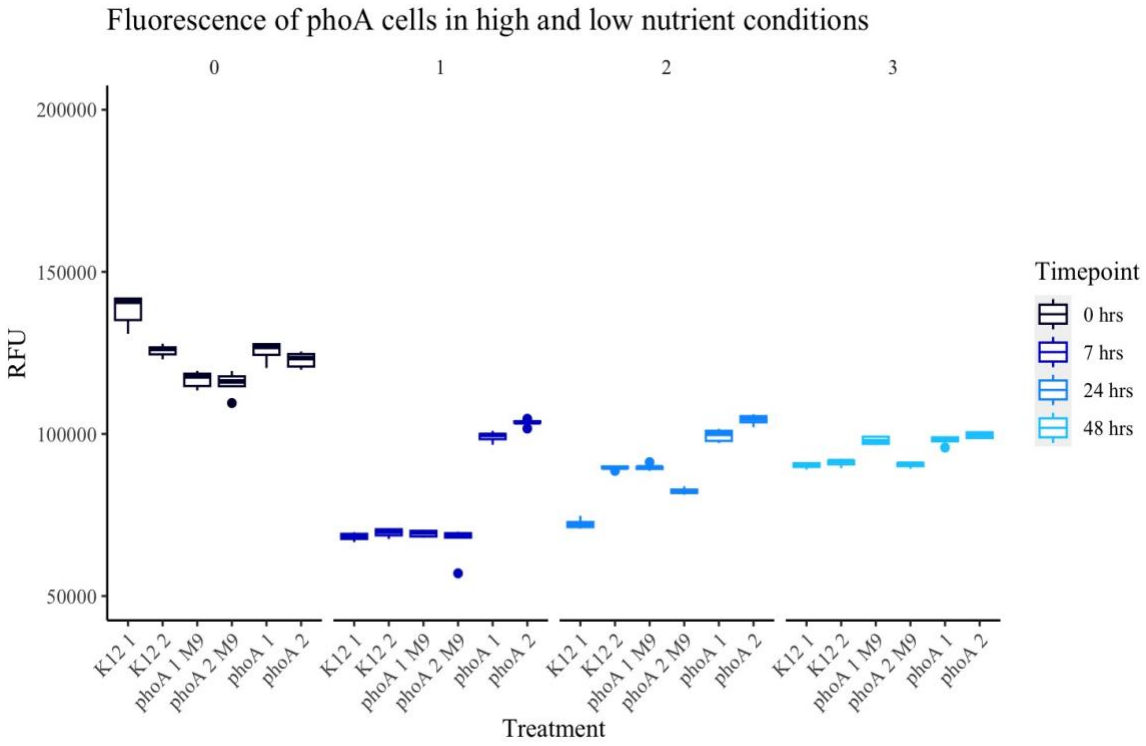

Figure 17. Boxplots of the fluorescence of *pho*A cells in liquid culture at high and low nutrient conditions. Fluorescence is in units of RFU and was normalized to OD before plotting. Outliers are represented by dots. (n=6). *Pho*A cells in low nutrient media fluoresced the highest at 7 and 24 hours, but after 7 hours *pho*A cells in high nutrient media began to fluoresce.

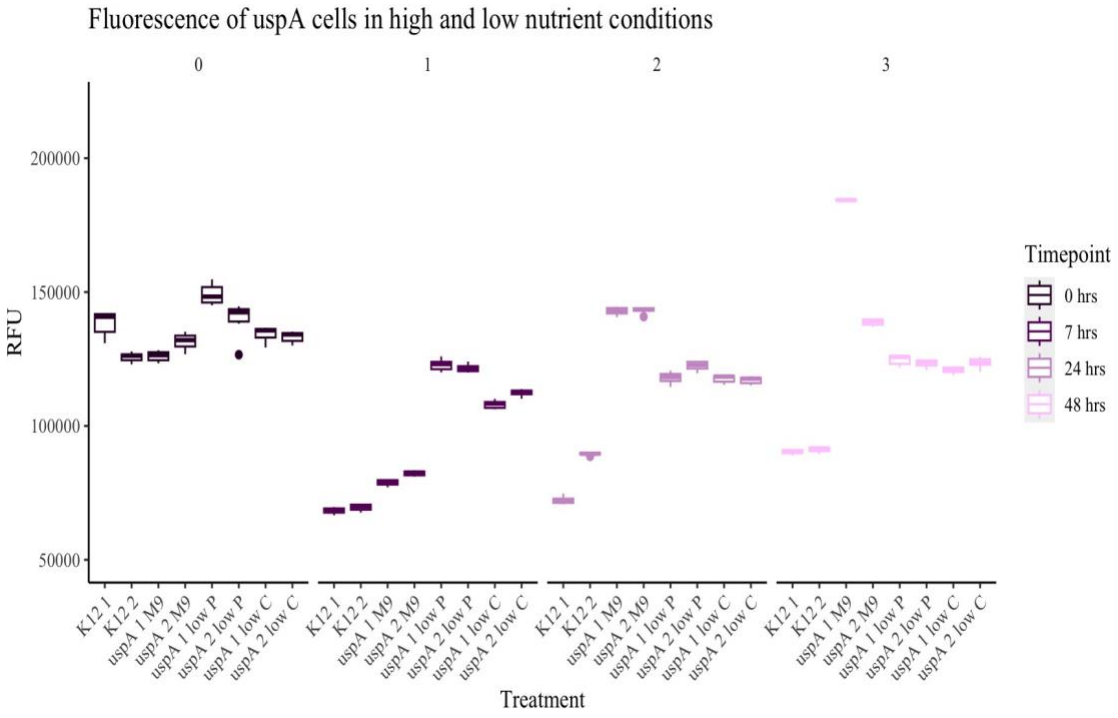

Figure 18. Boxplots of the fluorescence of *usp*A cells in liquid culture at high and low nutrient conditions. Fluorescence is in units of RFU and was normalized to OD before plotting. Outliers are represented by dots. (n=6). *Usp*A cells in low nutrient media fluoresced at 7, 24, and 48 hours, but after 7 hours *usp*A cells in high nutrient media began to fluoresce.

Construct response to nutrient limitation in sand

The molecular response of *gln*A and *csi*D constructs was examined further by deploying them separately in microcosms. The highest fluorescence was observed for *gln*A in low nutrient sand (284646 ± 65254 RFU). This was significantly higher than *gln*A in high nutrient sand (46084 ± 7340) and K12 (131737 ± 13768) at $p<0.0001$ and $p<0.05$, respectively. The Fluorescence of *gln*A in low nutrient sand was about 6 (6.18) times higher than *gln*A fluorescence in high nutrient sand and 2 (2.16) times higher than K12 fluorescence, as shown in

Figure 19. This was the biggest observed difference in RFU for liquid validation and sand microcosm experiments.

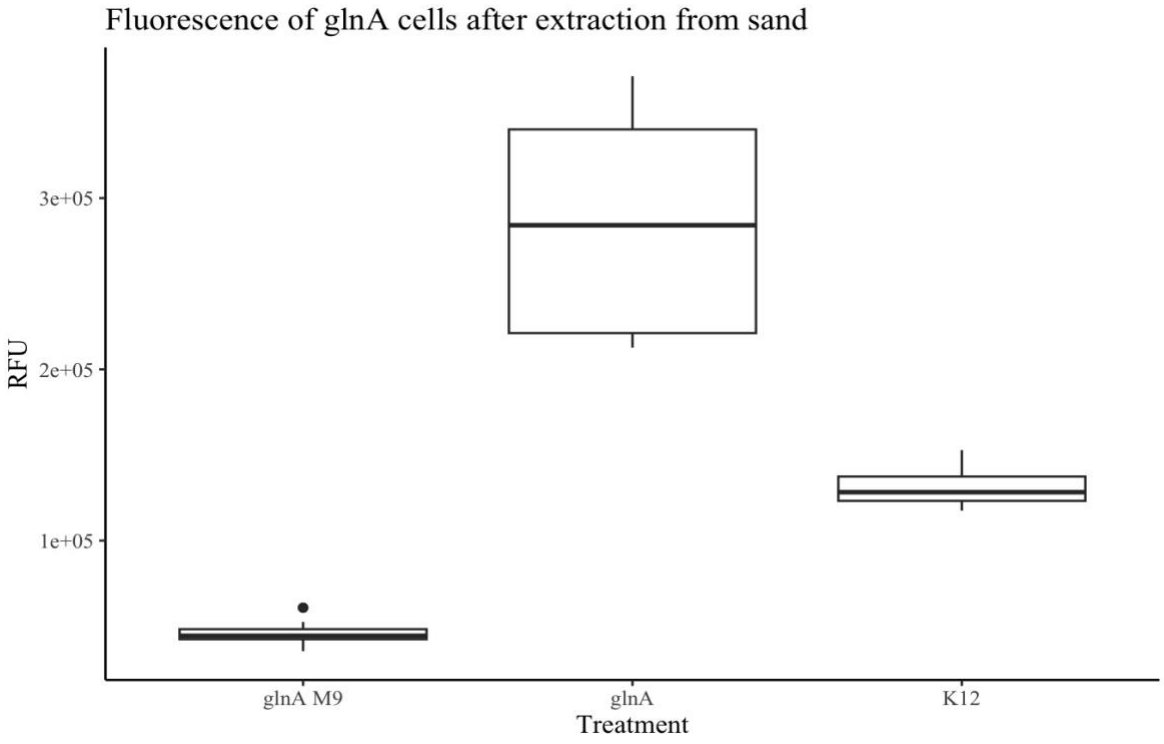

Figure 19. Fluorescence of *gln*A cells after 20 hours in sand . Fluorescence is in units of RFU and was corrected to OD before plotting (n=6). Outliers are represented by black dots. *Gln*A cells in low nutrient sand fluoresced about 6 times higher than *gln*A cells in higher nutrient sand and about 2 times higher than K12 at $p<0.5$.

The average fluorescence observed for *csi*D in low nutrient sand was lower than *gln*A in low nutrient sand (196086 ± 52123 RFU) but it was found to be significantly higher than the fluorescence observed for *csi*D in high nutrient sand (79906 ± 11650 RFU) and K12 (47869 ± 4096 RFU) at $p<0.05$. The fluorescence of *csi*D in low nutrient sand was about 2.5-fold (2.45) higher than the fluorescence of *csi*D in high nutrient sand and 4-fold (4.10) higher than the fluorescence of K12, as shown in Figure 20.

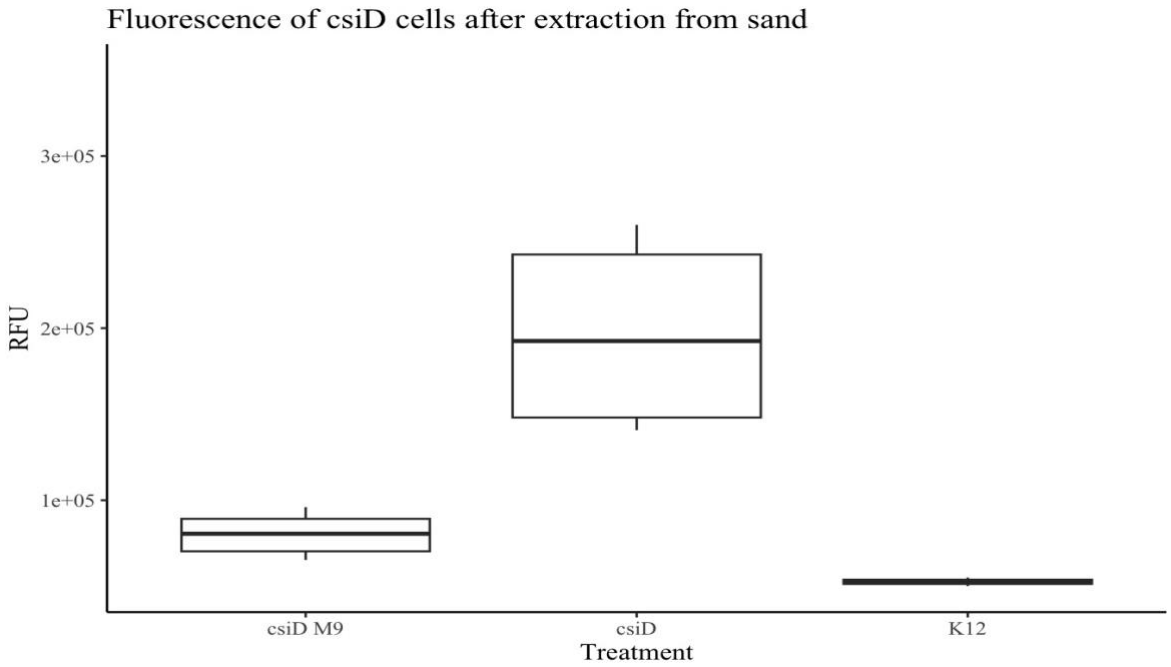

Figure 20. Fluorescence of *csi*D cells after 5 hours in sand. Fluorescence is in units of RFU and was corrected to OD before plotting (n=6). *Csi*D cells in low nutrient sand fluoresced about 2 times higher than *gln*A cells in higher nutrient sand and about 4 times higher than K12 at $p<0.5$.

3.4 Discussion

In the second chapter of this study we investigated larger-scale patterns in *E. coli* survival in the beach environment by sampling six Wisconsin beaches during the Summer of 2023. We used culture-based methods to enumerate *E. coli* concentrations in berm sand and surface water. In addition, we determined the concentrations of carbon, nitrogen, and phosphorus in the collected sand and water samples to determine if there was a correlation between *E. coli* burdens and nutrient concentration. In this chapter, we used this data to further investigate *E. coli* survival in beach sand by observing the molecular mechanism behind its survival using *E. coli* reporter constructs that produce GFP in response to nutrient limitation in laboratory microcosms. We extensively validated the constructs and determined that sand is, in general, a nutrient-deficient

environment for *E. coli*. Now that the constructs are validated, they have the potential to be used to evaluate the molecular response of *E. coli* in higher nutrient environments as well. This is important when evaluating sources of pollution at beaches that could add nutrients to the sand environment and prolong *E. coli* survival.

Do the constructs respond to nutrient limitation?

According to the sequencing results, GFP was correctly inserted into all of the constructs. We were not able to find the promoter region sequences for all the constructs, so we were not able to align those. However, the other validation experiments preformed indicate that the constructs do produce more GFP under nutrient stressed conditions compared to higher nutrient conditions. The fluorescence of all the constructs in low nutrient media is higher than the constructs in high nutrient media and K12 at 5-7 hours after initial deployment. After this time, the fluorescence of constructs in high nutrient media increases, indicating that the cells become nutrient stressed after 7 hours but before 24 hours. Out of all the constructs, *gln*A produces higher amounts of GFP in all conditions. Compared to *csi*D, *pho*A, and *usp*A in low nutrient liquid media at 7 hours, the fluorescence of *gln*A in low nutrient media is about 2 times higher. This could be because the *gln*A construct that was used was in a different host strain than the other constructs, which may have influenced the amount of GFP that the construct produces (Prasad et al, 2005).

However, compared to JM109:GFP, which produces GFP at constitutively at high levels, *gln*A produces significantly less GFP. During microcosms with the constructs, the gain that was used to measure the fluorescence was set to 95-100 while it had to be set to 75 for the JM109 extraction because the fluorescence overflowed the machine at higher gains. Now that the

constructs are extensively validated, it may be beneficial to transform *E. coli* cells that are found in Wisconsin freshwater sand, such as B1 cells, with the construct inserts to better represent a natural beach environment for future microcosm experiments. The constructs used for this study are typical laboratory *E. coli* strains, which means they are not well adapted to live in non-ideal or harsh environments.

Can the E. coli constructs be used in the sand-model system?

Extensive validation showed that the constructs respond to nutrient limitation in liquid media and in the sand environment. In addition, GFP production by *gln*A and *csi*D can be reduced by increasing the nutrient concentration in the sand through the addition of nitrogen and carbon containing solutions. During the validation of *gln*A in sand, nutrients were added in the form of M9 media. The concentration of nitrogen added to the high nutrient sand was 0.9347 μg/g sand. This is more than double the average amount of dissolved nitrogen at EICH, which had the highest overall TDN. This amount of additional nitrogen was sufficient to prevent *gln*A cells from fluorescing after 20 hours in the sand. During the validation of *csi*D in sand, nutrients were added to the sand in the form of M9 media and a glucose solution. The concentration of carbon added to the high nutrient sand was 60.00 μg/g sand, which is about 4 times higher than the dissolved carbon concentration of BB sand, which had the highest amount of TDC. This was sufficient to prevent the *csi*D cells that were in high nutrient sand from fluorescing after 5 hours. This suggests that beach sand is typically a nutrient-deficient environment for *E. coli,* and that nutrient-stress response pathways are activated at the natural nutrient levels in sand.

To properly examine the molecular response of *gln*A and *csi*D simultaneously, future experimentation should use the protocol for a sand-model system described in Appendix D.

Observing the timeframe in which *gln*A and *csi*D constructs begin to initiate stress response pathways would help increase our understanding of how nitrogen and carbon specifically modulate *E. coli* survival in beach sand. In Meyers & McLellan (2022), high levels of nitrogen above beach concentrations lead to increased *E. coli* survival within the first two weeks of a 6-week microcosm, while high levels of carbon prolonged survival during the last four weeks of the microcosm. The combined effect of both nutrients at higher amounts than average beach sand prolonged *E. coli* survival at even higher levels than treatments with carbon or nitrogen alone. Using *gln*A and *csi*D in the sand-model system may help us interpret these results in terms of the molecular response of *E. coli*.

In addition, the effect of *Cladophora* on the molecular response of *E. coli* to nutrient stress in sand could be investigated using the sand-model system. It would be interesting to deploy microcosms with the constructs and *Cladophora* mat additions and see how the constructs respond over time. In Meyers & McLellan (2022) the addition of *Cladophora* mats to microcosms significantly decreased the decay rate of *E. coli*. In addition, decayed *Cladophora* mats had less potential to increase the survival of *E. coli* in the sand. Simultaneously deploying *gln*A, *csi*D and *pho*A in microcosms with fresh and decayed *Cladophora* and evaluating the relative fluorescence intensities could shed light on the mechanism by which the algae provide nutrients to the bacteria. This could have large implications on beach management practices, since some beach management programs groom beaches and remove *Cladophora* mats and other programs do not.

Chapter 4- Conclusions

Prolonged survival of *E. coli* in beach sand confounds current beach monitoring efforts that rely on *E. coli* enumeration in surface water. Through wave action, the *E. coli* that is deposited in berm sand is continuously mixed with the nearby surface water through wave action. Culture-based methods for FIB enumeration, which are routinely used by beach management programs in the Great Lakes region, cannot determine the source of the pollution or when a pollution event may have occurred. Not knowing the source of the FIB makes it difficult for beach managers evaluate the threat that the beach environment poses to public health because some sources of fecal pollution, such as human sewage, are more dangerous to public health than other sources. It can also lead to unnecessary closures of beaches due to elevated bacteria levels.

Understanding the underlying mechanisms behind *E. coli* survival in secondary environments such as beach sand, especially in the context of nutrient provision, is poorly understood but is important to informing culture-based water quality assessments at beaches. Our study routinely sampled six Wisconsin beaches throughout the summer of 2023 to determine *E. coli* and nutrient concentrations in the beach environment. Overall, there were no significant differences among beaches in terms of *E. coli* or nutrient concentrations. However, patterns in larger scale regional factors such as average summer rainfall can affect *E. coli* exceedance and advisory incidences at Wisconsin beaches. In addition, there are some beaches that are "hot spots" for high *E. coli* and nutrient concentrations due to smaller-scale regional factors including beach size, construction features such as breakwaters, and proximity to rivers carrying water polluted by agricultural runoff. We intended to further examine some of these "hot spot" beaches, especially beaches with high nutrient concentrations, through microbial community analysis using the filters prepared in Chapter 2.2 of this study to examine how nutrient

availability may modulate the native community. Although we were not able to use the filters in this study, they will be stored in the McLellan lab for future beach environment research.

Our study also investigated the molecular response of *E. coli* to nutrient limitation in the beach environment. We extensively validated *E. coli* reporter constructs that consist of GFP inserted next to promoters that control pathways that respond to nutrient limitation. The reporter constructs that respond to carbon, nitrogen, and phosphorus produce a measurable GFP signal when exposed to nutrient limitation, which is significantly higher than the level of GFP production at higher nutrient levels. Constructs that respond to carbon and nitrogen limitation were validated further through deploying them in laboratory microcosms. Nutrient data acquired in the first part of this study helped interpret the amount of carbon and nitrogen that is needed to prevent GFP production, which is two to four times higher than beach levels. This suggests that the beach is generally a nutrient-deficient environment for *E. coli*, although further experimentation should be done with fresh sand collected during the summer. There is also potential for the constructs to be used to evaluate the molecular response of *E. coli* in higher nutrient conditions. In future studies, it would be beneficial to use the constructs in microcosms to determine the underlying mechanism with which the freshwater algae *Cladophora* provide nutrients to *E. coli*. This is especially informative for beach management practices and could shed light on how quickly *Cladophora* mats should be removed from beaches.

REFERENCES

1. Abia ALK, Ubomba-Jaswa E, Momba MNB. 2015. Impact of seasonal variation on Escherichia coli concentrations in the riverbed sediments in the Apies River, South Africa. Science of the Total Environment 537:462–469.

2. Alm EW, Burke J, Hagan E. 2006. Persistence and potential growth of the fecal indicator bacteria, Escherichia coli, in shoreline sand at Lake Huron. Journal of Great Lakes Research 32:401-405.

3. Beaches Environmental Assessment and Coastal Health Act, 33 U.S.C. §1313 et seq. (2000). chrome-extension://efaidnbmnnnibpcajpcglclefindmkaj/https://www.congress.gov/106/plaws/publ284/PLAW-106publ284.pdf

4. Beckinghausen A, Martinez A, Blersch D, Haznedaroglu BZ. 2014. Association of nuisance filamentous algae Cladophora spp. with E. coli and Salmonella in public beach waters: Impacts of UV protection on bacterial survival. Environmental Sciences: Processes and Impacts 16:1267-1274.

5. Beversdorf LJ, Bornstein-Forst SM, McLellan SL. 2007. The potential for beach sand to serve as a reservoir for Escherichia coli and the physical influences on cell die-off. Journal of Applied Microbiology 102:1372-1381.

6. Bootsma H. 2004. Cladophora Research and Management in the Great Lakes.

7. Brown KI, Boehm AB. 2016. Transport of fecal indicators from beach sand to the surf zone by recirculating seawater: laboratory experiments and numerical modeling. Environmental Science and Technology 50:12840-12847.

8. Byappanahalli MN, Shively DA, Nevers MB, Sadowsky MJ, Whitman RL. 2003. Growth and survival of Escherichia coli and enterococci populations in the macro-alga Cladophora (Chlorophyta). FEMS Microbiology Ecology 46:203-211.

9. Cloutier DD, Alm EW, McLellan SL. 2015. Influence of land use, nutrients, and geography on microbial communities and fecal indicator abundance at Lake Michigan beaches. Applied and Environmental Microbiology 81:4904-4913.

10. Cloutier DD, McLellan SL. 2017. Distribution and differential survival of traditional and alternative indicators of fecal pollution at freshwater beaches. Applied and Environmental Microbiology 83.

11. Cold Spring Harbor Protocols. 2010. M9 minimal medium (standard). Cold Spring Harbor protocols. http://cshprotocols.cshlp.org/content/2010/8/pdb.rec12295.short

12. Cold Spring Harbor Protocols. 2006. M9 salts. Cold Spring Harbor Protocols. http://cshprotocols.cshlp.org/content/2006/1/pdb.rec614.short

13. Edge T, Hill S. 2007. Multiple lines of evidence to identify the sources of fecal pollution at a freshwater beach in Hamilton Harbour, Lake Ontario. Water Research 41:3585-3594.

14. Field KG, Samadpour M. 2007. Fecal source tracking, the indicator paradigm, and managing water quality. Elsevier Ltd 41:3517-3538.

15. Geider R & La Roche J. 2002. Redfield revisited: variability of C:N:P in marine microalgae and its biochemical basis. European Journal of Phycology 37: 1-17.

16. Haack SK, Fogarty LR, Wright C. Escherichia coli and enterococci at beaches in the Grand Traverse Bay, Lake Michigan: sources, characteristics, and environmental pathways. Environmental science & technology 37(15):3275-82.

17. Harwood VJ, Staley C, Badgley BD, Borges K, Korajkic A. 2014. Microbial source tracking markers for detection of fecal contamination in environmental waters: Relationships between pathogens and human health outcomes. 38:1-40.

18. Ishii S, Hansen DL, Hicks RE, Sadowsky MJ. 2007. Beach sand and sediments are temporal sinks and sources of Escherichia coli in Lake Superior. Environmental Science and Technology 41:2203-2209

19. Kleinheinz GT, McDermott CM, Hughes S, Brown A. 2009. Effects of rainfall on E. coli concentrations at Door County, Wisconsin beaches. International Journal of Microbiology 2009.

20. Kumwimba MN, Meng F, Oluwayinka I, Moore MT, Bo Z, Tao W, Liang TJ, Ilunga L. 2018. Removal of non-point source pollutants from domestic sewage and agricultural runoff by vegetated drainage ditches (VDDs): Design, mechanism, management strategies, and future directions. Science of the Total Environment 639:742-759.

21. Magee, M.R., Packett, D.L., 2022. Wisconsin's Great Lakes Beach Monitoring & Notification Program 2021 Beach Season Summary. Report # 3900-2022-04. Wisconsin Department of Natural Resources.

22. Mandel MJ, Silhavy TJ. 2005. Starvation for different nutrients in Escherichia coli results in differential modulation of RpoS levels and stability. Journal of Bacteriology 187:434-442.

23. McLellan SL, Prasad G. Mechanisms and management of E. coli accumulation in beach sand.

24. McLellan SL, Salmore AK. 2003. Evidence for localized bacterial loading as the cause of chronic beach closings in a freshwater marina. Water Research 37:2700-2708.

25. Meyers, Brigid. 2022. Influence of Nutrients and the Native on E. Coli Survival in the Beach Environment. Theses and Dissertations. 2923. https://dc.uwm.edu/etd/2923

26. Meyers BC, McLellan SL. 2022. Influence of Nutrients and the Native Community on E. Coli Survival. Applied and Environmental Microbiology. *88*(21) e01043-22.

27. National Weather Service. NOWData-NOAA Online Weather Data. Retrieved March 30, 2024. NOAA https://www.weather.gov/wrh/Climate?wfo=mkx.

28. Odonkor ST, Ampofo JK. 2013. Escherichia coli as an indicator of bacteriological quality of water: an overview. Microbiology Research 4:2-2.

29. Passante EK, Dechant LE, Paradis CJ, McLellan SL. 2022. Halophilic bacteria in a Lake Michigan drainage basin as potential biological indicators of chloride-impacted freshwaters. Science of the Total Environment 846.

30. Phillips MC, Solo-Gabriele HM, Piggot AM, Klaus JS, Zhang Y. Relationships between sand and water quality at recreational beaches. Water Research 20: 6763-6769.

31. Prasad G, Paliy O, McAuliffe J, Popham D, Jordan M, Kustu S. 2005. Sulfur and nitrogen limitation in Escherichia coli K-12: Specific homeostatic responses. Journal of Bacteriology 187:1074-1090.

32. Roguet A, Esen ÖC, Murat Eren A, Newton RJ, McLellan SL. 2020. FORENSIC: an Online Platform for Fecal Source Identification.

33. Rumball NA, Mayer HRC, McLellan SL. 2021. Selective Survival of Escherichia coli Phylotypes in Freshwater Beach Sand. Applied and Environmental Microbiology 87.

34. Safaie A, Weiskerger CJ, Nevers MB, Byappanahalli MN, Phanikumar MS. 2021. Evaluating the impacts of foreshore sand and birds on microbiological contamination at a freshwater beach. Water Research 190.

35. Scopel CO, Harris J, McLellan SL. Influence of nearshore water dynamics and pollution sources on beach monitoring outcomes at two adjacent Lake Michigan beaches. Journal of Great Lakes Research 32:543-52.

36. Shanks OC, Kelty CA, Oshiro R, Haugland RA, Madi T, Brooks L, Field KG, Sivaganesan M. 2016. Data acceptance criteria for standardized human-associated fecal source identification quantitative real-time PCR methods. Applied and Environmental Microbiology 82:2773-2782.

37. Skalbeck J, Kinzelman J, Mayer G. 2010. Fecal indicator organism density in beach sands: Impact of sediment grain size, uniformity, and hydrologic factors on surface water loading. Journal of Great Lakes Research. 36:707–714.

38. Somorin Y, Abram F, Brennan F, O'Byrne C. 2016. The general stress response is conserved in long-term soil-persistent strains of Escherichia Coli. Applied and Environmental Microbiology 82:4628-4640.

39. Staley ZR, Edge TA. 2016. Comparative microbial source tracking methods for identification of fecal contamination sources at Sunnyside Beach in the Toronto region area of concern. Journal of Water and Health 14:839-850.

40. Staley ZR, He DD, Shum P, Vender R, Edge TA. 2018. Foreshore beach sand as a reservoir and source of total phosphorus in Lake Ontario. Aquatic Ecosystem Health and Management 21:268-275.

41. Stainton, M.P., Capel M.J., Armstrong F.A.J. I977. The Chemical Analysis of Fresh Water, 2nd ed. Can. Fish. Mar. Serv. Misc. Spec. Publ. 25: I80 p

42. Templar HA, Dila DK, Bootsma MJ, Corsi SR, McLellan SL. 2016. Quantification of human-associated fecal indicators reveal sewage from urban watersheds as a source of pollution to Lake Michigan. Water Research 100:556-567.

43. US EPA. (2012). Recreational water quality criteria. Health and Ecological Criteria Division OoSaT. 42.

44. Vogel LJ, O'Carroll DM, Edge TA, Robinson CE. 2016. Release of Escherichia coli from Foreshore Sand and Pore Water during Intensified Wave Conditions at a Recreational Beach. Environmental Science and Technology 50:5676-5684.

45. Walk ST, Alm EW, Calhoun LM, Mladonicky JM, Whittam TS. 2007. Genetic diversity and population structure of Escherichia coli isolated from freshwater beaches. Environmental Microbiology 9:2274-2288.

46. Walker, D.I., McQuillan, J., Taiwo, M., Parks, R., Stenton, C.A., Morgan, H., Mowlem, M.C. and Lees, D.N., 2017. A highly specific Escherichia coli qPCR and its comparison with existing methods for environmental waters. Water Research. 126:101-110.

47. Whitman RL, Nevers MB. 2008. Summer *E. coli* Patterns and Responses along 23 Chicago Beaches. Environmental Science & Technology 42: 9217–9224

48. Whitman RL, Nevers MB. 2003. Foreshore sand as a source of Escherichia coli in nearshore water of a Lake Michigan Beach. Applied and Environmental Microbiology 69:5555-5562.

49. Winfield MD, Groisman EA. 2003. Role of nonhost environments in the lifestyles of Salmonella and Escherichia coli, vol 69, p 3687-3694.

50. Wisconsin DNR. n.d. Beach Monitoring Program Requirements. https://dnr.wisconsin.gov/sites/default/files/topic/Beaches/BeachMonitoringRequirements.pdf

51. Wisconsin DNR. 2023. Beach Reports. Retrieved March 13, 2024. https://apps.dnr.wi.gov/beachhealth/

52. Wisconsin DNR. Impaired Water Search. Retrieved March 13, 2024. https://apps.dnr.wi.gov/water/impairedsearch.aspx?name=beach

53. Wisconsin DNR. Kenosha County Beaches on Lake Michigan [map]. May, 2017. 1:60,000. https://dnr.wisconsin.gov/sites/default/files/topic/Beaches/maps/Kenosha.pdf

54. Wisconsin DNR. Milwaukee County Beaches on Lake Michigan [map]. December, 2015. 1:135,000. https://dnr.wisconsin.gov/sites/default/files/topic/Beaches/maps/Milwaukee.pdf

55. Wisconsin DNR. 2023. Nitrogen in Northeast Lakeshore TMDL study area. https://dnr.wisconsin.gov/sites/default/files/topic/TMDLs/NEL/NE_Lakeshore_Nitrogen_Analysis.pdf

56. Wisconsin DNR. 2023. The Northeast Lakeshore TMDL: Total maximum daily loads for total phosphorus and total suspended solids. Appendix H. https://dnr.wisconsin.gov/sites/default/files/topic/TMDLs/NEL_TMDL_report_approved.pdf

57. Wisconsin DNR. Ozaukee County Beaches on Lake Michigan [map]. December, 2017. 1:150,000. https://dnr.wisconsin.gov/sites/default/files/topic/Beaches/maps/Ozaukee.pdf

58. Wisconsin DNR. 2023. Wisconsin Beach List. https://dnr.wisconsin.gov/sites/default/files/topic/Beaches/2023_WIBeachList.pdf

59. Wisconsin's Great Lakes Beach Monitoring & Notification Program 2020 Beach Season Summary. December 16, 2021. Wisconsin Department of Natural Resources.

60. Wisconsin's Great Lakes Beach Monitoring & Notification Program 2019 Beach Season Summary. December 17, 2020. Wisconsin Department of Natural Resources.

61. Zaslaver, A. Bren, A., Ronen, M., Itzkovitz1, S., Kikoin, I., Seagull Shavit, S., Liebermeister, W., Surette, M., Alon, U. 2006. A comprehensive library of fluorescent transcriptional reporters for Eschericia coli. Nat Methods 3, 623-628 https://doi.org/10.1038/nmeth895

62. Zehms T, McDermott C, Kleinheinz G. 2008. Microbial Concentrations in Sand and their Effect on Beach Water in Door County, Wisconsin. Journal of Great Lakes Research. 34:524–534.

63. Zhang L, Huang S, Peng X, Liu B, Zhang X, Ge F, Zhou Q, Wu Z. 2021. Potential ecological implication of Cladophora oligoclora decomposition: Characteristics of nutrient migration, transformation, and response of bacterial community structure. Water Research 190.

Appendix A- Beach sampling data

Date	Beach	Sample type	Average *E. coli* count (CFU/100 mL or CFU/g)	Average TDC (mg/L or µg/g)	Average DOC (mg/L or µg/g)	Average TDN (mg/L or µg/g)
05-24-2023	BB	Water	252.0	NA	NA	NA
05-24-2023	BB	Sand	40.79	NA	NA	NA
05-30-2023	HAR	Water	0.0000	NA	NA	NA
05-30-2023	HAR	Sand	0.6848	NA	NA	NA
05-30-2023	PWSB	Water	4.000	NA	NA	NA
05-30-2023	PWSB	Sand	0.1953	NA	NA	NA
06-05-2023	BB	Water	2.667	NA	NA	NA
06-05-2023	BB	Sand	12.13	NA	NA	NA
06-07-2023	ATW	Water	85.50	NA	NA	NA
06-07-2023	ATW	Sand	131.1	NA	NA	NA
06-08-2023	EICH	Water	33.33	NA	NA	NA
06-08-2023	EICH	Sand	14.15	NA	NA	NA
06-08-2023	SIMM	Water	8.333	NA	NA	NA
06-08-2023	SIMM	Sand	4.135	NA	NA	NA
06-12-2023	ATW	Water	34.75	NA	NA	NA
06-12-2023	ATW	Sand	2.429	NA	NA	NA
06-12-2023	BB	Water	30.33	NA	NA	NA
06-12-2023	BB	Sand	6.212	NA	NA	NA
06-13-2023	EICH	Water	18.00	NA	NA	NA
06-13-2023	EICH	Sand	12.03	NA	NA	NA
06-13-2023	SIMM	Water	9.333	NA	NA	NA
06-13-2023	SIMM	Sand	0.9922	NA	NA	NA
06-15-2023	HAR	Water	71.00	NA	NA	NA
06-15-2023	HAR	Sand	22.48	NA	NA	NA
06-15-2023	PWSB	Water	24.67	NA	NA	NA
06-15-2023	PWSB	Sand	9.854	NA	NA	NA
06-20-2023	ATW	Water	8.500	19.85	2.231	0.318
06-20-2023	ATW	Sand	1.334	15.99	2.443	0.124
06-20-2023	BB	Water	0.3333	24.11	2.238	0.370
06-20-2023	BB	Sand	3.446	20.25	2.693	0.224

Date	Beach	Sample type	Average *E. coli* count (CFU/100 mL or CFU/g)	Average TDC (mg/L or µg/g)	Average DOC (mg/L or µg/g)	Average TDN (mg/L or µg/g)
06-21-2023	ATW	Water	6.250	24.31	1.880	0.365
06-21-2023	ATW	Sand	10.062	14.92	1.472	0.519
06-21-2023	BB	Water	6.000	25.74	1.926	0.354
06-21-2023	BB	Sand	10.38	14.97	1.285	0.479
06-26-2023	EICH	Water	6.667	25.55	2.533	0.453
06-26-2023	EICH	Sand	228.1	19.37	2.974	0.569
06-26-2023	SIMM	Water	10.33	25.74	1.911	0.410
06-26-2023	SIMM	Sand	5.025	19.46	1.269	0.309
06-27-2023	HAR	Water	401.2	20.29	1.556	0.303
06-27-2023	HAR	Sand	1106.	9.894	1.175	0.605
06-27-2023	PWSB	Water	410.4	18.85	1.539	0.324
06-27-2023	PWSB	Sand	3.406	13.22	0.8580	0.185
06-28-2023	EICH	Water	28.67	21.03	1.633	0.360
06-28-2023	EICH	Sand	30.88	18.40	1.196	0.330
06-28-2023	SIMM	Water	14.67	20.10	1.182	0.246
06-28-2023	SIMM	Sand	6.880	17.10	1.399	0.336
06-29-2023	HAR	Water	55.33	24.80	1.304	0.415
06-29-2023	HAR	Sand	5.486	8.964	0.0000	0.284
06-29-2023	PWSB	Water	10.00	24.96	1.238	0.408
06-29-2023	PWSB	Sand	1.173	14.06	0.3648	0.401
07-11-2023	ATW	Water	44.25	23.97	1.875	0.312
07-11-2023	ATW	Sand	8.383	9.392	0.7500	0.109
07-11-2023	BB	Water	108.3	26.26	1.943	0.322
07-11-2023	BB	Sand	5.699	12.70	1.309	0.342
07-13-2023	ATW	Water	81.00	27.73	0.9939	0.199
07-13-2023	ATW	Sand	8.154	11.19	0.4724	0.139
07-13-2023	BB	Water	32.00	19.22	0.9628	0.190
07-13-2023	BB	Sand	11.06	19.03	1.209	0.161
07-17-2023	EICH	Water	519.3	23.56	2.139	0.420
07-17-2023	EICH	Sand	707.7	9.321	2.012	0.460
07-17-2023	SIMM	Water	21.00	20.22	2.239	0.444
07-17-2023	SIMM	Sand	109.4	6.398	1.230	0.165

Date	Beach	Sample type	Average *E. coli* count (CFU/100 mL or CFU/g)	Average TDC (mg/L or µg/g)	Average DOC (mg/L or µg/g)	Average TDN (mg/L or µg/g)
07-18-2023	HAR	Water	8.333	25.24	1.491	0.309
07-18-2023	HAR	Sand	0.8846	10.85	1.459	0.711
07-18-2023	PWSB	Water	9.667	24.94	1.743	0.411
07-18-2023	PWSB	Sand	3.883	14.56	0.8994	0.241
07-19-2023	EICH	Water	136.3	24.43	1.993	0.403
07-19-2023	EICH	Sand	475.4	15.62	1.622	0.146
07-19-2023	SIMM	Water	25.33	25.34	2.158	0.403
07-19-2023	SIMM	Sand	276.4	14.19	1.732	
07-20-2023	HAR	Water	21.67	24.56	1.951	0.438
07-20-2023	HAR	Sand	0.7705	11.81	1.311	0.208
07-20-2023	PWSB	Water	22.33	25.35	2.186	0.453
07-20-2023	PWSB	Sand	14.13	10.96	1.205	0.270
07-24-2023	ATW	Water	35.75	23.60	2.231	0.423
07-24-2023	ATW	Sand	3.471	15.59	6.130	0.285
07-24-2023	BB	Water	48.67	24.26	2.294	0.428
07-24-2023	BB	Sand	7.572	17.41	6.565	0.318
07-26-2023	ATW	Water	325.8	24.70	1.874	0.404
07-26-2023	ATW	Sand	897.2	9.399	0.7138	0.184
07-26-2023	BB	Water	32.00	25.46	2.046	0.429
07-26-2023	BB	Sand	268.4	11.79	1.245	0.364
07-31-2023	HAR	Water	20.00	23.90	1.984	0.323
07-31-2023	HAR	Sand	11.59	3.439	0.8974	0.369
07-31-2023	PWSB	Water	5.333	23.60	1.985	0.415
07-31-2023	PWSB	Sand	2.615	5.413	1.192	0.104
08-01-2023	EICH	Water	71.33	24.93	1.946	0.377
08-01-2023	EICH	Sand	590.9	14.65	1.643	0.447
08-01-2023	SIMM	Water	57.00	25.70	2.030	0.355
08-01-2023	SIMM	Sand	12.19	9.427	1.382	0.313
08-02-2023	HAR	Water	620.3	27.93	2.019	0.231
08-02-2023	HAR	Sand	3.377	20.411	4.791	0.225
08-02-2023	PWSB	Water	16.33	26.023	1.966	NA
08-02-2023	PWSB	Sand	0.9933	20.90	2.162	0.078
08-03-2023	EICH	Water	20.00	24.60	1.7600	0.350

Date	Beach	Sample type	Average *E. coli* count (CFU/100 mL or CFU/g)	Average TDC (mg/L or µg/g)	Average DOC (mg/L or µg/g)	Average TDN (mg/L or µg/g)
08-03-2023	EICH	Sand	55.14	5.883	1.409	0.603
08-03-2023	SIMM	Water	56.67	22.72	1.826	0.358
08-03-2023	SIMM	Sand	14.01	4.272	1.064	0.243
08-07-2023	ATW	Water	91.00	26.36	2.025	0.384
08-07-2023	ATW	Sand	55.16	14.23	0.6243	0.061
08-07-2023	BB	Water	29.33	27.44	2.222	0.431
08-07-2023	BB	Sand	8.158	16.30	1.163	0.105
08-08-2023	ATW	Water	9.250	23.34	1.979	0.409
08-08-2023	ATW	Sand	1.659	12.33	1.388	0.196
08-08-2023	BB	Water	19.67	24.00	2.031	0.432
08-08-2023	BB	Sand	1.176	10.56	1.699	0.333
08-28-2023	HAR	Water	17.67	26.58	2.063	0.400
08-28-2023	HAR	Sand	3.880	10.38	1.210	0.056
08-28-2023	PWSB	Water	3.667	26.16	2.0409	0.418
08-28-2023	PWSB	Sand	0.5506	14.50	1.490	0.156
08-29-2023	EICH	Water	65.67	25.91	2.042	0.459
08-29-2023	EICH	Sand	12.24	8.567	1.732	0.377
08-29-2023	SIMM	Water	9.667	26.19	1.891	0.295
08-29-2023	SIMM	Sand	2.612	10.58	1.313	0.222

Date	Beach	Sample type	Average TDP (ug/g sand)
06-21-2023	BB	Sand	0.029
06-21-2023	ATW	Sand	0.038
06-26-2023	EICH	Sand	0.023
06-26-2023	SIMM	Sand	0.015
06-27-2023	PWSB	Sand	0.015
06-27-2023	HAR	Sand	0.061
07-13-2023	BB	Sand	0.014
07-13-2023	ATW	Sand	0.014
07-17-2023	EICH	Sand	0.018
07-17-2023	SIMM	Sand	0.015
07-18-2023	HAR	Sand	0.056
07-18-2023	PWSB	Sand	0.024
07-20-2023	HAR	Sand	0.017
07-20-2023	PWSB	Sand	0.013
07-24-2023	BB	Sand	0.022
07-24-2023	ATW	Sand	0.033
08-03-2023	SIMM	Sand	0.018
08-03-2023	HAR	Sand	0.034
08-08-2023	BB	Sand	0.037
08-08-2023	ATW	Sand	0.028
08-38-2023	HAR	Sand	0.049
08-28-2023	PWSB	Sand	0.017
08-29-2023	EICH	Sand	0.029
08-29-2023	SIMM	Sand	0.018

MilliQ Blank date	Average TDC (mg/L)	Average DOC (mg/L)	Average TDN (mg/L)
06-20-2023	3.113	0.3748	-0.011
06-21-2023	2.715	0.3649	0.06994
06-26-2023	2.472	0.2984	0.0468
06-27-2023	1.006	0.2082	0.01512
06-28-2023	2.755	0.2252	0.0737
06-29-2023	2.72	1.004	0.07316
07-12-2023	1.396	0.5435	0.1262
07-13-2023	1.949	0.4334	0.1152
07-17-2023	0.5097	0.3789	0.03305
07-18-2023	1.821	0.2898	-0.007925
07-19-2023	1.676	0.3044	-0.01855
07-20-2023	1.575	0.1557	-0.007845
07-24-2023	0.4305	0.2395	0.01758
07-26-2023	0.4611	0.4532	0.06631
07-31-2023	0.5113	0.4061	0.04991
08-01-2023	0.1743	0.1896	0.05745
08-02-2023	0.2365	0.2935	0.08156
08-03-2023	0.5304	0.4143	0.06603
08-07-2023	0.307	0.5143	0.01956
08-08-2023	0.3087	0.2698	0.01235
08-28-2023	0.326	0.2424	-0.02394
08-29-2023	0.3279	0.221	0.0184

Appendix B- Spatial variation of *E. coli* and nutrient variability between sites at Simmons Island Beach in Kenosha

Summary

For every sampling event, sand was collected at several sites and used as biological replicates for the beach. Three sites were sampled at each beach except for Atwater Park Beach, which had four sites. To investigate small-scale variation in *E. coli* and nutrient concentrations in the sand at a beach, Simmons Island Beach in Kenosha was sampled. Sites were located along the length of the beach and at different depths (Figure S.1.1). The *E. coli*, dissolved organic, and total dissolved nitrogen concentrations at each site were not found to be significantly different from each other among sites at $p<0.5$. The total dissolved carbon concentration at Sites 1 was found to be significantly higher than Site 3, but the p-value was barely below 0.05 with post hoc analysis ($p=0.0481$). For this reason, and because all other sites were not found to be significantly different from each other, we decided to use sites as biological replicates for sampling events for data analysis purposes.

Methods

Simmons Island Beach was sampled on August 16, 2023. At each site, three sand subsamples were collected and named according to Table 1. The 3 subsamples were collected approximately 1 meter apart from each other parallel to the shore. Sand was also collected at different depths below the surface at Site 2 at approximately 10 cm down (Site 4) and approximately 17 cm down (Site 5). Figure 1 is a representation of the location of the samples taken from Simmons Island Beach. In total 15 samples were collected. Each sample processed and analyzed using the methods outlined in Chapter 2.

Table 1. Subsamples collected at each site at Simmons Island Beach. Sites 1, 2, and 3 are the sites described in Chapter 2.1 while Sites 4 & 5 are located at different depths bellow Site 2. Site 4 is 10.16 cm down and Site 5 is 16.764 cm down.

Site	Subsamples
1	7, 8, 9
2	4a, 5a, 6a
3	1, 2, 3
4	10b, 11b, 12b
5	13c, 14c, 15c

Results

The median *E. coli* concentrations increased from northern to southern sites and from the surface of the sand to the deepest site according to Figures 2 & 3. Site 1 had the lowest median concentration at 2.257 CFU/ g dry sand while Site 5 had the highest median concentration at 3.083 CFU/g dry sand. *E. coli* concentrations at sites were not found to be significantly different from each other among Sites 1, 2, & 3 along with Sites 2, 4, & 5 at the level of $p<0.05$ using multiple analysis of variance tests.

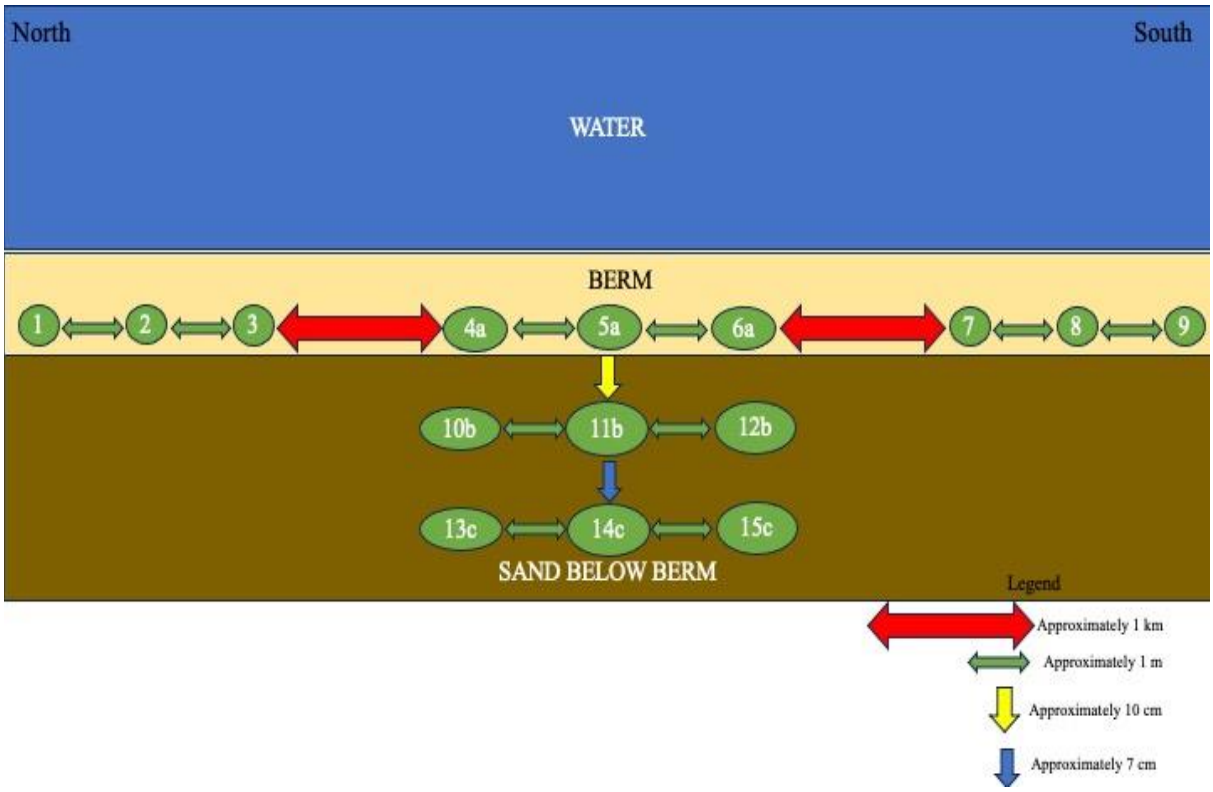

Figure 1. Map of the location of subsamples collected at Simmons Island Beach on 8/16/2023.

Total dissolved carbon, organic carbon, and nitrogen concentrations also increased from northern to southern sites, but not from the surface of the sand to the deepest site according to Figures 4 & 5. Median total dissolved carbon concentrations decreased from Site 2 to 4 while total dissolved organic carbon and nitrogen concentrations decreased from Site 2 to 4 and increased from Site 4 to 5. Subsample 14c, located in Site 5, had a total dissolved carbon concentration of 78.27 ug/g dry sand. This high of a concentration was not seen in sand at any of the sampled beaches in Chapter 2 so it was omitted from the analysis due to likely contamination.

There were significant differences in nutrient concentrations among Sites 1, 2, and 3 at $p<0.05$ ($p=0.043$). Site 3 had a significantly higher total dissolved carbon concentration than Site 1 using Tukey's post hoc analysis ($p=0.0481$). There were no significant differences in dissolved organic carbon and total dissolved nitrogen concentrations among Sites 1, 2, and 3 at $p<0.05$. There also was no significant differences in nutrient concentrations among Sites 2, 4, and 5 at $p<0.05$.

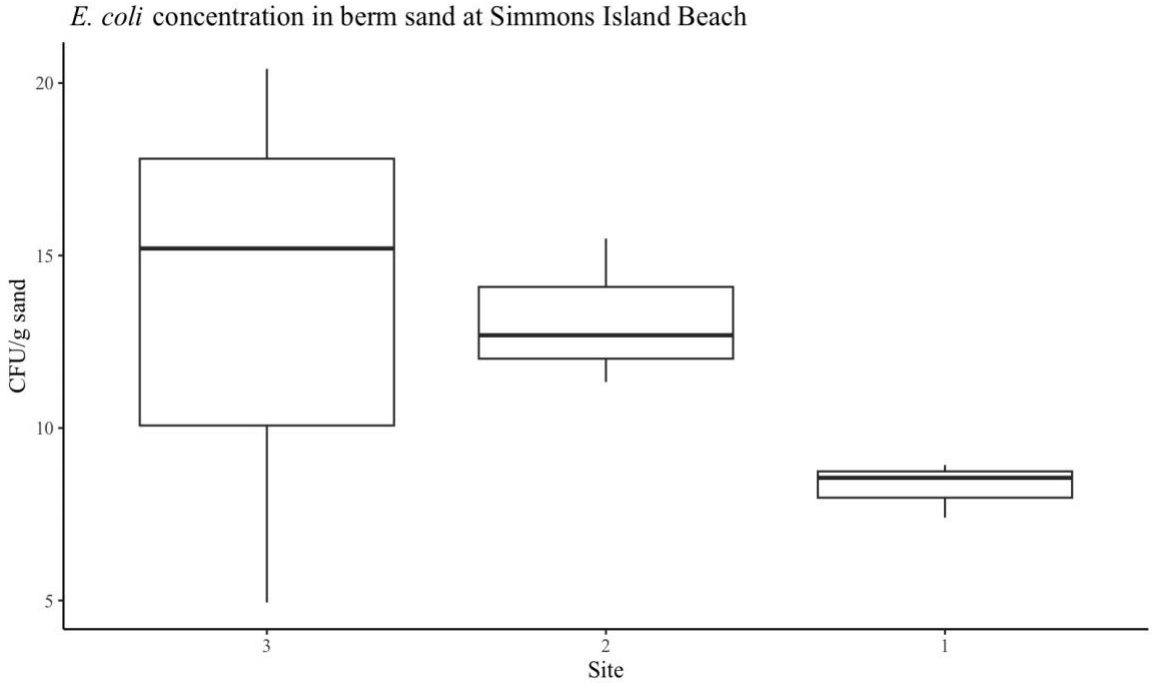

Figure 2. Boxplot of the *E. coli* concentrations in berm sand at Sites 1, 2, and 3 at Simmons Island Beach. *E. coli* concentrations are in units of CFU per gram of dry sand and were log-transformed before plotting. Site 1 is the most southern site while Site 3 is the most northern site at the beach.

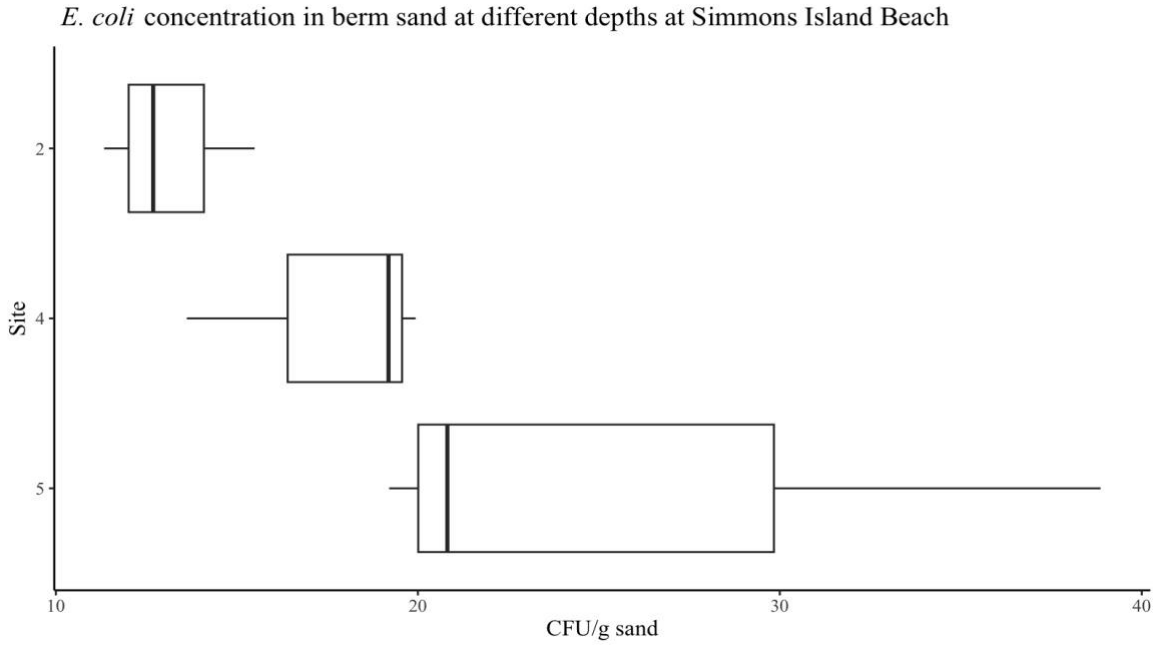

Figure 3. Boxplot of the *E. coli* concentrations in berm sand at Sites 1, 2, 3, 4, & 5 at Simmons Island Beach. *E. coli* concentrations are in units of CFU per gram of dry sand and were log-transformed before plotting. Site 2 is the site at the surface while Sites 4 and 5 are at different depths bellow Site 2.

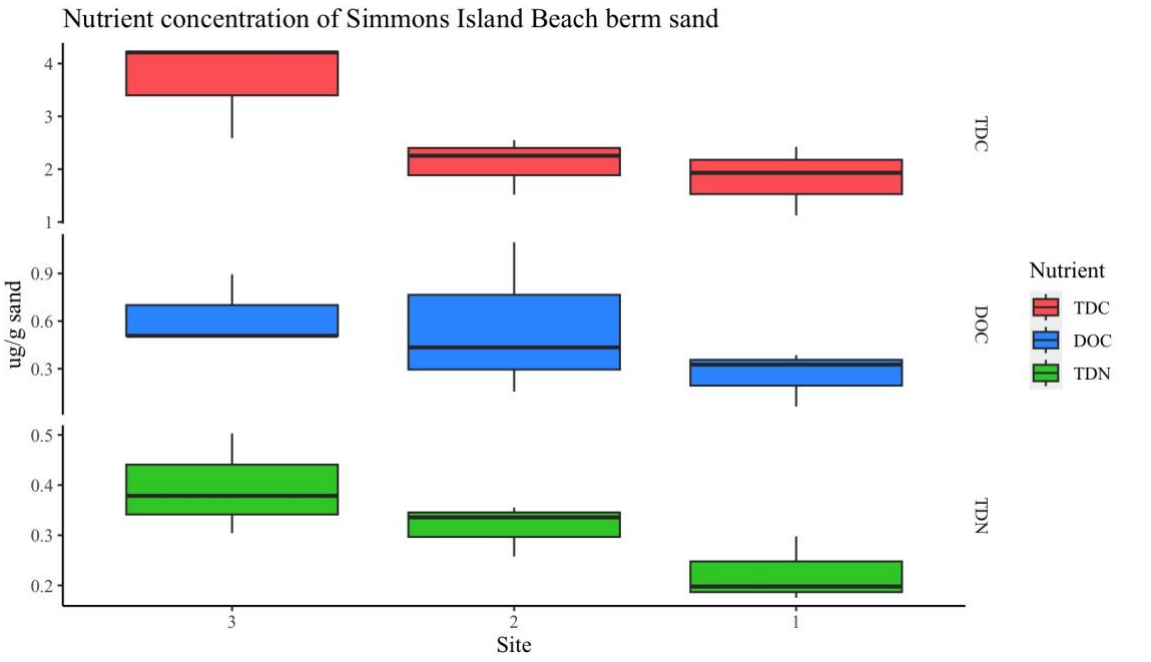

Figure 4. Boxplots of nutrient concentrations at Sites 1, 2, & 3 at Simmons Island Beach. Nutrient concentrations are in units of microgram per gram of dry sand. Site 1 is the most southern site while Site 3 is the most northern site at the beach.

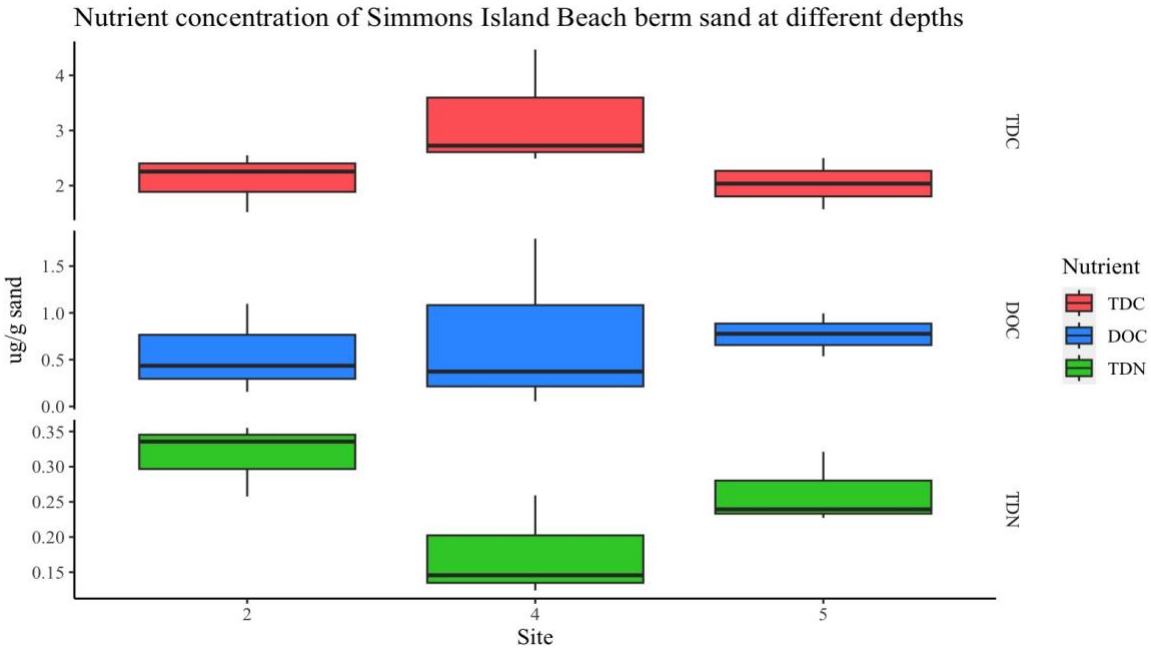

Figure 5. Boxplots of nutrient concentrations at Sites 2, 4, & 5 at Simmons Island Beach. Nutrient concentrations are in units of microgram per gram of dry sand. Site 2 is the most southern site while Site 3 is the most northern site at the beach. Site 2 is at the surface while Sites 4 & 5 are at different depths bellow Ste 2. Subsample 14c was omitted from analysis due to likely contamination.

Appendix C: Medias for *E. coli* GFP construct validation

M9 salt solution (250 mL)[1]

Stock	Weight
$Na_2HPO_4 \bullet 7\ H_2O$	16 g
KH_2PO_4	3.75 g
NaCl	0.625 g
NH_4Cl	1.25 g

Mix the solution in between each reagent addition.
Autoclave at 121°C for 15 minutes on a liquid cycle.

Full Strength M9 media (50 mL)[1]

Stock	Weight
M9 salt solution	10 mL
1 M $MgSO_4$	200 μL
20 % glucose solution	1 mL
5M $CaCl_2$	1 μL
Sterile H_2O	38.799 mL

M9 salt solution, no nitrogen (250 mL)[1]

Stock	Weight
$Na_2HPO_4 \bullet 7\ H_2O$	16 g
KH_2PO_4	3.75 g
NaCl	0.625 g

Mix the solution in between each reagent addition.
Autoclave at 121°C for 15 minutes on a liquid cycle.

Low nitrogen M9 media (50 mL)[1]

Stock	Weight
M9 solution, no nitrogen	9.456 mL
M9 salt solution	535μL
1 M $MgSO_4$	200 μL
20 % glucose solution	1 mL
5M $CaCl_2$	1 μL
Sterile H_2O	38.799 mL

M9 salt solution, no phosphorus (250 mL)[1]

Stock	Weight
NH_4Cl	1.25 g
NaCl	0.625 g

Mix the solution in between each reagent addition.
Autoclave at 121°C for 15 minutes on a liquid cycle.

Low phosphorus M9 media (50 mL)[1]

Stock	Weight
M9 solution, no phosphorus	9.998 mL
M9 salt solution	2 μL
1 M $MgSO_4$	200 μL
20 % glucose solution	1 mL
5M $CaCl_2$	1 μL
Sterile H_2O	38.799 mL

Low carbon M9 media (50 mL)[1]

Stock	Weight
M9 salt solution	10 mL
1 M $MgSO_4$	200 μL
20 % glucose solution	100 μL
5M $CaCl_2$	1 μL
Sterile H_2O	39.699 mL

NH_4Cl solution (250 mL)[1]

Stock	Weight
NH_4Cl	1.25 g
Sterile H_2O	250 mL

[1]Adapted from Cold Spring Harbor Protocols, 2010 and Cold Spring Harbor Protocols, 2006.

Appendix D: Ideal sand-model system protocol with *E. coli* GFP constructs

Summary

To examine the molecular responses of two of the *E. coli* reporter constructs used in this study, *gln*A and *csi*D, they were deployed simultaneously in a microcosm and extracted at several different timepoints. The constructs in high nutrient sand fluoresced more than the constructs in low nutrient sand at the first timepoint, which was five hours after they were deployed. In future microcosms, sand should be collected in the summer months and used in microcosms close to when it is collected to prevent loss of the native microbial community and prevent the constructs from becoming stressed early on in the microcosm due to poor sand conditions. Therefore, there is potential for this sand-model system to be improved and modified to further examine how nutrients modulate *E. coli* survival in beach sand.

Methods

E. coli K12 cells were used as a negative control in the microcosm. High nutrient sand and low nutrient sand treatment groups were prepared in triplicate. Both *gln*A and *csi*D along with K12 were grown from single colonies in M9 media shaking overnight at 37 °C and 250 rpm. Microcosms were prepped according to the protocol in Chapter 3.2. For high nutrient sand with *gln*A cells, 3 mL of an NH_4Cl solution was added (Appendix C). For high nutrient sand with *csi*D cells, 80 μL 20% glucose was added to 450 g sand. M9 media was also added to K12 sand (Appendix C). Sterile water was also added to all treatment groups to adjust the sand moisture. Reporter construct and K12 cells were extracted according to the protocol in Chapter 3.2 under the section titled “Microcosms with *E. coli* GFP reporter constructs”.

The fluorescence excitation was set to 485 nm and the emission was at 535 nm with the gain set to 95. The sand was processed at 4 hours, 20 hours, and 44 hours after the cultures were seeded into the sand. The OD was measured using a clear 96-well plate and the fluorescence was measured in a black and white 96-well isoplate. using a Synergy H4 Multi-mode Reader. The wavelength was set to 600 nm for OD readings while the fluorescence excitation was set to 485 nm and the emission was to 535 nm with the gain at 75. The fluorescence of K12 for timepoint 2 was not obtained because the wrong cells were measured during analysis. The data displayed in the graph is from previous validation experiments where the fluorescence of K12 was measured after extraction from sand at 22-24 hours.

Results

The fluorescence of all treatments generally increased after every extraction. At 5 hours, the average fluorescence of *gln*A in high nutrient sand was 178147 RFU, which was significantly higher than *gln*A in low nutrient sand and K12 at $p<0.05$ (Figure 1). At 5 hours, the fluorescence of *csi*D in high nutrient sand was 244027 RFU, and was only slightly higher than *csi*D in low nutrient sand and K12 (Figure 2). At 22-24 hours, the fluorescence of *gln*A and *csi*D in low nutrient sand increased compared to 5 hours. *Gln*A in low nutrient sand was significantly higher than *gln*A in high nutrient sand while *csi*D in low nutrient sand was significantly lower than *csi*D in high nutrient sand at $p<0.0005$. By 46-48 hours the fluorescence of the constructs in low nutrient sand was higher than the constructs in high nutrient sand, but the difference was only significant for *gln*A at $p<0.0001$. The fluorescence of K12 also increased dramatically and was nearly identical to *gln*A in high nutrient media as well as surpassing the fluorescence of *csi*D in high and low nutrient sand significantly at $p<0.0005$ and $p<0.05$, respectively.

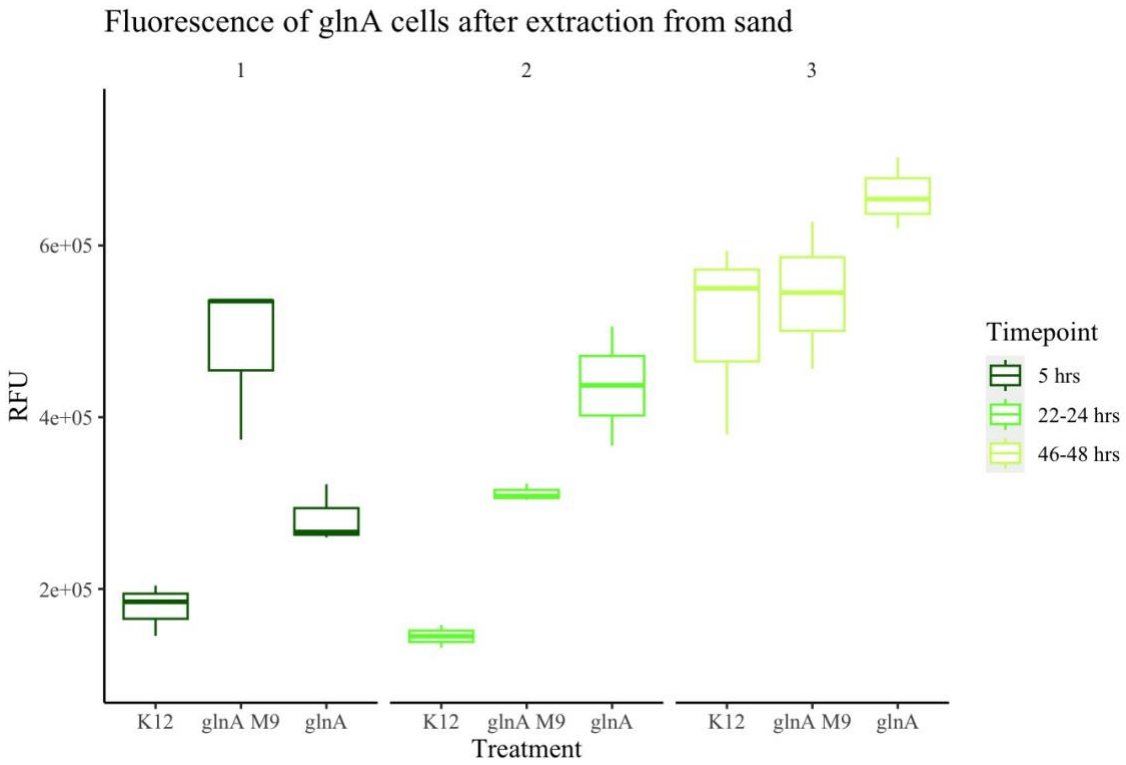

Figure 1. Fluorescence of *gln*A cells in high and low nutrient sand. Each boxplot represents triplicate replicates. Fluorescence is in units of relative fluorescence units and was normalized to OD before plotting.

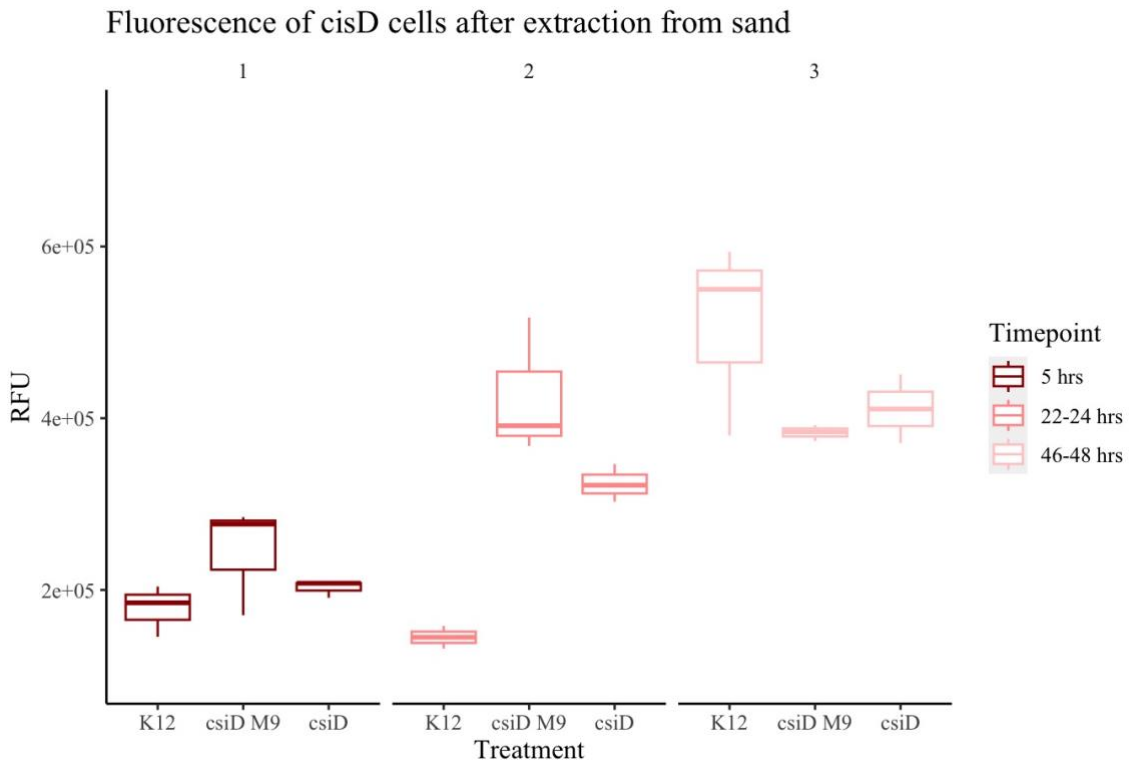

Figure 2. Fluorescence of *csi*D cells in high and low nutrient sand. Each boxplot represents triplicate replicates. Fluorescence is in units of relative fluorescence units and was normalized to OD before plotting.

Discussion

The constructs that were in high nutrient sand fluoresced more than the constructs in low nutrient sand 5 hours after deployment, indicated in Figures 1 & 2. This may be because of the condition of the sand that was used for the microcosms. The sand was collected from BB on December 5, 2023, before any significant snowfalls in the area. The sand was then kept in the fridge at 4 °C until use on January 10th, 2024. By this time the sand had been in the fridge for over a month, but new sand was not acquired because of weather constraints.

Samples for nutrient analysis were prepared directly before the sand was used to check for carbon and nitrogen concentrations. Interestingly, later nutrient analysis using the Shimadzu TOC analyzer showed that the sand contained a higher concentration of TDC, DOC, and TDN

than the average concentrations for BB in the summer. BB sand collected in December had a TDC concentration of 20.74 μg/g sand, a DOC concentration of 2.240 μg/g sand, and a TDN concentration of 0.5831 μg/g sand. Although the nutrient concentrations increased, the extended storage time in the fridge and the condition that the sand was stored in (in whirlpacks) most likely greatly affected the native microbial community in the sand, which was most likely less active than it was in the summer when it was collected. *E. coli* enumeration in the sand when it was collected showed a concentration of 0 CFU/g sand. The sealed whirlpacks, although not airtight, also prevented gas exchange with the environment. This most likely lead to a buildup of gases such as ethylene, which is poisonous to many microbes.

To properly examine the molecular response of *gln*A and *csi*D simultaneously the microcosms should be repeated during the summer months, when the weather is warmer, and sand can be collected easily. This will prevent long-term storage of the sand before deployment in microcosms, and the sand will have a more robust native community. In addition, the molecular responses of *pho*A and *usp*A could be examined further in microcosms. TDP data acquired in this study would help determine how much additional phosphorus should be added to sand for high nutrient sand treatments.

Ideal sand-model system protocol

Further experimentation using the sand-model system described in this Appendix should use the following protocol:

- Collect berm sand from a nearby beach and process it according to the methods described in Section 2.2. Preferably sand should be collected during a warm summer month, such as July or August. A significant amount of sand should be collected (at least 5 kg).

- Culture at least 50-100 mLs of the desired constructs and K12 in M9 media overnight, shaking at 250 rpm. For the reporter construct cultures, add kanamycin to a final concentration of 25 μg/ mL.
- The next day, determine the cell concentration of each culture.
- Weigh out 580 g of sand two times for each construct and put it into clean plastic bins. Label the bins with each construct name and either high or low nutrients.
- Weigh out another 580 g of sand and put it into a separate, clean bin. Label this bin with K12.
- Add the cultures to the sand to a final concentration of 10^7 cells/g sand. Homogenize the sand by shaking the bins or mixing the sand with a clean plastic utensil.
- Add nutrients to the high nutrient media in the form of M9 media. Depending on the the sand, the final amount of liquid added to the sand to maintain a typical moisture content for berm sand may vary. However, at least 2 times more nitrogen and 4 times more carbon should be added to high nutrient sand for the *gln*A and *csi*D treatment groups. Extra nitrogen and carbon, on top of the M9 media, can be added in the form of the NH_4Cl solution and a 20% glucose solution described in Appendix C. A smaller validation experiment should be done with *pho*A in the sand-model system to determine how much phosphorus should be added to the high nutrient sand before deployment in a larger microcosm.
- Homogenize the sand again.
- Label 35 mm x 10 mm petri dishes with the treatment name and timepoint. There should be at least 3-4 timepoints.

- Fill the petri dishes with sand completely and use a flat edged scooper to even out the top of the sand.
- Place the petri dishes in clean microcosm chambers (See Section 3.2) and keep them in a fridge set to 18 °C until processing.
- Process the dishes in the first timepoint immediately after weighing them into petri dishes according to Section 2.2.
- During processing for each timepoint, make sure to measure the absorbance at 600 nm and the fluorescence at an excitation of 395 nm and emission of 510 nm. Measure the fluorescence at each timepoint at several different gains. For example, measure the fluorescence of each treatment at gains of 75, 80, 85, 90, 95, and 100. Excessively high fluorescence can overload the machine, preventing the machine from reporting a fluorescence. Measuring the fluorescence at several different gains ensures that the machine will not be overloaded and that all readings from each timepoint are measured at the same gain if the fluorescence increases over the course of the experiment.